Neutron Scattering Investigation of Phase Transitions and Magnetic Correlations in the Two-Dimensional Antiferromagnets K_2NiF_4, Rb_2MnF_4, Rb_2FeF_4

R. J. BIRGENEAU
Bell Telephone Laboratories, Murry Hill, New Jersey 07974
and Brookhaven National Laboratory, Upton, New York 11973*

AND

H. J. GUGGENHEIM
Bell Telephone Laboratories, Murry Hill, New Jersey 07974

AND

G. SHIRANE
Brookhaven National Laboratory, Upton, New York 11973*

(Received 9 October 1969)

The quasi-elastic magnetic scattering from the planar antiferromagnets K_2NiF_4, Rb_2MnF_4, Rb_2FeF_4 has been studied over a wide range of temperatures both above and below the phase transition. In all three compounds the diffuse scattering above the phase transition takes the form of a *ridge* rather than a *peak*, thus giving the first concrete evidence for the two-dimensional nature of the magnetism. At T_N (97.1, 38.4, 56.3°K, respectively), the crystals undergo sharp phase transitions to long-range order (LRO) in three dimensions. For $0.002 \leq 1-T/T_N \leq 0.1$, the sublattice magnetizations in K_2NiF_4 and Rb_2MnF_4 follow a $(T_N-T)^\beta$ law with $\beta=0.14$ and 0.16, respectively. Rb_2MnF_4 is found to have two distinct magnetic phases, both with identical ordering within the planes but with different stacking arrangements of the spins between planes; both phases are found to have identical T_N's and β's to within the experimental accuracy of 0.1°K. The sublattice magnetization in Rb_2FeF_4 has a rather more complicated behavior, apparently due to magnetostrictive effects. Finally, in the ordered phase in each compound, the three-dimensional magnetic Bragg peaks are accompanied by "diffuse" scattering which is completely two-dimensional in form. These results are discussed in terms of a model in which the phase transition is viewed as being essentially two-dimensional in character, the three-dimensional ordering simply following as a necessary consequence of the onset of LRO with the planes. The systems therefore should have distinct two- and three-dimensional critical regions. The three-dimensional region apparently was not experimentally accessible with 0.1°K temperature control in K_2NiF_4 and Rb_2MnF_4, indicating that in these compounds $|T/T_N-1|_3 \leq 2\times10^{-3}$.

I. INTRODUCTION

SINCE Onsager's famous work,[1] the two-dimensional ([2]) Ising model has occupied a unique position in the theory of cooperative phenomena. It is the only system exhibiting a phase transition for which exact results are available. In Onsager's work and in subsequent explorations by other authors it was shown that the "classical" theories were wholly incapable of accounting for the properties of the [2] Ising system. More recently, considerable theoretical attention has been directed towards the [2] Heisenberg model. Stanley and Kaplan[2] showed that the extrapolation techniques which have been so successful in predicting the properties of three-dimensional ([3]) systems seem to indicate a divergence in the susceptibility for the [2] Heisenberg model at a temperature approximately one-half the corresponding molecular field value. This was thought to be in contradiction with spin-wave theory which predicts that no long-range order (LRO) is possible for $T>0$. Shortly after Stanley and Kaplan's hypothesis appeared, however, Mermin and Wagner[3] supplied an exact proof that both the Heisenberg magnet and the axial transverse magnet ($|J_x|=|J_y|=|J_\perp|>|J_\parallel|$) cannot display a spontaneous magnetization if the interactions are of finite range. Thus the Stanley-Kaplan transition must be to a state with very long-range correlations but no true LRO. Finally, using the random-phase approximation (RPA) Green's-function technique, Lines has shown that the [2] Heisenberg model is extremely sensitive to anisotropy.[4] Indeed, even minute amounts are apparently enough to lift the spontaneous-magnetization phase-transition temperature from 0°K to an appreciable fraction of the molecular field value.

Although all of these results and speculations on [2] systems are clearly very interesting, it has always appeared that they are largely of academic value. For example, the main role which Onsager's solution of the [2] Ising model has played, aside from showing that the theory of phase transitions lies within the realm of equilibrium statistical mechanics, is as a testing ground for the approximation developed by the theorists for [3] systems.[5] Recently, however, it has been suggested that systems which approximate [2] antiferromagnets very closely do indeed exist in

* Work performed under the auspices of the U. S. Atomic Energy Commission.

[1] L. Onsager, Phys. Rev. 65, 117 (1944).

[2] H. E. Stanley and T. A. Kaplan, Phys. Rev. Letters 17, 913 (1966).

[3] N. D. Mermin and H. Wagner, Phys. Rev. Letters 17, 1133 (1966).

[4] M. E. Lines, Phys. Rev. 164, 736 (1967).

[5] For a review of the theory see M. E. Fisher, Rept. Progr. Phys. 30, 615 (1967).

nature.[4,6] The prototype for these is K_2NiF_4, a planar analog of the perovskite $KNiF_3$. The first magnetic experiments carried out on this family of compounds were bulk susceptibility measurements by Srivastava.[7] He found that the susceptibilities were characterized by broad maxima followed by a discontinuity in $\chi_\perp$, typically at $\sim\frac{1}{2}T_{\chi\,\max}$, where $T_{\chi\,\max}$ is the temperature at which χ achieves its maximum value. Neutron diffraction experiments on *powdered* K_2NiF_4 were carried out by Plumier.[6] He observed a rather anomalous temperature dependence of the magnetic superlattice line intensities and widths. On the basis of these results together with some consideration of the magnetic symmetry, he concluded that the perovskite NiF_2 planes ordered within themselves at 180°K, but that even at 4.2°K there was no true LRO between the planes. It would appear therefore that K_2NiF_4 is a genuine [2] antiferromagnet. Since Plumier's work, a number of investigations have been carried out on the bulk properties of K_2NiF_4 itself[8,9] and of isotructural compounds such as K_2MnF_4,[10] Rb_2MnF_4,[10] K_2CoF_4,[11] and Rb_2FeF_4.[12] In each case, the susceptibilities have a common shape and indeed, on this basis, arguing by analogy with K_2NiF_4, the authors have tended to conclude that the other compounds are also [2] antiferromagnets.

It seems clear that if Plumier's conjecture is correct, then experiments on these compounds could yield results of considerable importance to our understanding of cooperative phenomena, particularly in the critical region. Recently, we have succeeded in growing large single crystals of K_2NiF_4, Rb_2FeF_4, and Rb_2MnF_4. We have therefore undertaken a comprehensive study of their properties using elastic and inelastic neutron scattering techniques. In this paper, we present the results of the first phase of this program. This work, therefore, is largely a groundwork study in which we attempt to characterize the basic properties of these

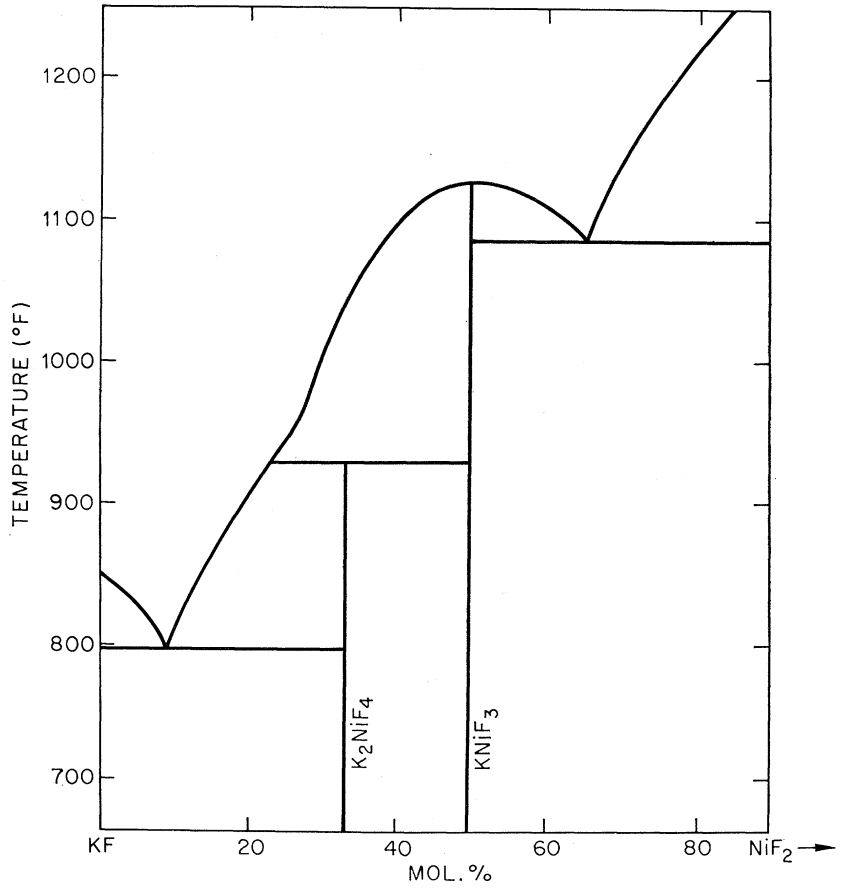

FIG. 1. KF-NiF_2 chemical-phase diagram.

[6] R. Plumier, J. Appl. Phys. **35**, 950 (1964); J. Phys. (Paris) **24**, 741 (1963).
[7] K. V. Srivastava, Phys. Letters **4**, 55 (1963).
[8] E. P. Maarschall, A. C. Botterman, S. Vega, and A. R. Miedema, Physica **41**, 473 (1969).
[9] J. S. Tiwari, A. Mehra, K. G. Srivastava, J. Appl. Phys. (Japan) **7**, 506 (1968).
[10] D. J. Breed, Physica **37**, 35 (1967).
[11] V. J. Folen, J. J. Krebs, and M. Rubenstein, Solid State Commun. **6**, 865 (1968).
[12] G. K. Wertheim, H. J. Guggenheim, H. J. Levinstein, D. N. E. Buchanan, and R. C. Sherwood, Phys. Rev. **173**, 614 (1968).

compounds and, in particular, their two-dimensionality, with more detailed experiments employing precise resolution corrections to follow at a later date. We should note that a brief report of our K_2NiF_4 experiments has already appeared in the literature.[13]

The format of this paper is as follows. In Sec. II, we give preliminary details such as the crystallography, crystal growth, and magnetic structure, together with a discussion of the magnetism in each of the compounds. In Sec. III, we review the theory of magnetic neutron scattering, particularly as applied to two-dimensional systems. The experimental results are presented in Sec. IV and finally, in Sec. V, we propose a model to account for the experimental observations and then discuss the results in this context.

II. PRELIMINARY DETAILS

A. Grystal Crowth

Single crystals up to 1 cm^3 of K_2NiF_4, Rb_2MnF_4, and Rb_2FeF_4 have been grown from the melt using a horizontal-zone-melting method. The general direction of growth was normal to the c axis.

The phase-equilibria data obtained from the differential thermal analysis of these compounds suggest a strong similarity to the phase-equilibrium diagram of the KF-NiF_2 system as determined by Wagner and Balz.[14] This diagram (Fig. 1) shows the two-dimensional phase, K_2NiF_4, to be incongruently melting at 930°C. At this temperature the compound transforms to $KNiF_3$ and liquid. Single crystals of incongruently melting materials of this type can generally be grown by slow cooling the compound with an excess of one of its components, e.g., $2KF+NiF_2$ with an excess of KF. The crystals are, however, in the form of plates with the thin dimensions perpendicular to the c axis.

We have grown large bulk crystals of the two-dimensional phase using the horizontal-zone method. In this method a traveling molten zone with two liquid-solid interfaces allows the growth of separate phases to take place at different sections of the boat as the composition of the melt changes. For example, if a molten zone of approximately 2 cm is established at the beginning end of a 9-cm boat filled with $2\,KF\cdot NiF_2$, the first solid to form after an increment of travel would be the perovskite $KNiF_3$. When the composition of the zone changes sufficiently, the second phase, K_2NiF_4, begins to crystallize. In practice, we have found each phase to occupy approximately one-third of the boat when the starting composition does not contain an excess of either component. Work is now in progress on the effect of various starting compositions.

B. Crystallography and Magnetic Structure

The crystal structure of K_2NiF_4 together with that of $KNiF_3$ is given in Fig. 2. From the figure it may be seen that K_2NiF_4 is composed of simple cubic NiF_2 and KF planes identical to those in $KNiF_3$. However, the stacking arrangement of the planes in K_2NiF_4 differs from that in $KNiF_3$ and it is this which gives rise to the two-dimensionality. In K_2NiF_4, each successive NiF_2 plane is separated by two KF planes. In addition the Ni^{++} ion in nearest-neighbor (nn) planes are such that an ion in one plane is equidistant from *four* magnetic ions in the neighboring plane. At room temperature the edge of the cubic cell in $KNiF_3$ [15] is $a_0=4.014\pm0.001$ Å. The room-temperature dimensions of the K_2NiF_4 cell[16] are $a_0=4.006$ Å, $c_0=13.076$ Å. In both cases the Ni^{2+} cations are surrounded by an octahedron of fluorine ions. For K_2NiF_4, this octahedron may have a very small tetragonal distortion which will give rise to a small axial anisotropy. The crystal structures of Rb_2MnF_4 and Rb_2FeF_4 are identical to those of K_2NiF_4 although, of course, the fluorine and potassium (rubidium) positional parameters will differ

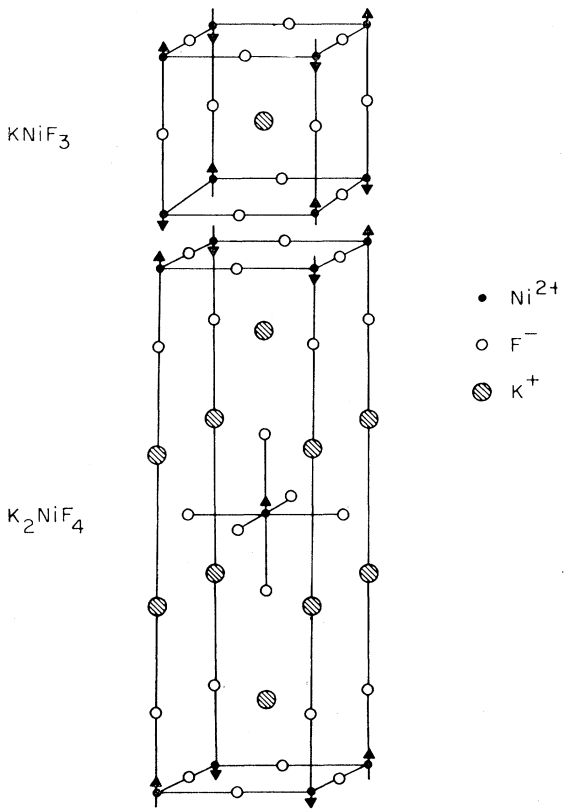

FIG. 2. Crystal structures for $KNiF_3$ and K_2NiF_4 showing the antiferromagnetic arrangement of the nickel spins as exhibited by these crystals in their magnetically ordered states.

[13] R. J. Birgeneau, H. J. Guggenheim, and G. Shirane, Phys. Rev. Letters 22, 720 (1969).
[14] G. Wagner and D. Balz, Z. Elektrochem. 56, 574 (1952).
[15] A. Okazaki and Y. Suemune, J. Phys. Soc. Japan 16, 671 (1961).
[16] D. Balz and K. Pleith, Z. Elektrochem. 59, 545 (1955).

TABLE I. Low-temperature lattice constants in K_2NiF_4, Rb_2MnF_4, Rb_2FeF_4.

	K_2NiF_4	Rb_2MnF_4	Rb_2FeF_4
T(°K)	80	4.2	55
a_0(Å)	3.994±0.004	4.20±0.01	4.214±0.008
c_0(Å)	13.04 ±0.01	13.77±0.04	13.53 ±0.02

somewhat. The low-temperature lattice constants determined in this study for all three compounds are given in Table I.

The magnetic structures of $KNiF_3$ [17] and K_2NiF_4 [18] are also shown in Fig. 2. As is well known, the magnetic structure of the transition-metal perovskites is determined by the strong antiferromagnetic superexchange which exists between nearest neighbors, so that the nn spins are always oriented antiparallel. As expected, this simple magnetic structure is carried over to the NiF_2 planes in K_2NiF_4. Here, however, there is an additional anisotropy term which fixes the spins along the c axis. With this structure within the planes, it may easily be seen that the net exchange field produced at the cation sites in the nn planes is exactly zero. Hence, to first order there is no interaction between adjacent planes in the Néel state. Indeed Lines[4] has shown that any interaction between the nn planes tends to inhibit ordering with the planes. Thus any LRO in the c direction must be established by the coupling between the next-nearest-neighbor (nnn) layers. In K_2NiF_4 this coupling is evidently so as to make the spins along the tetragonal axis parallel to each other. As we shall see later it is this effective decoupling of nn planes which makes the two-dimensional nature of these compounds much more pronounced than in other planar compounds, such as $CrBr_3$ [19] and $CrCl_3$.[20] It should be noted that a magnetic structure determination has also been carried out by Cox *et al.* on Ca_2MnO_4.[21] In this case, the ordering within the planes is identical to that in K_2NiF_4 but the nnn planes are oriented such that successive spins along the c axis are antiparallel. We shall discuss the magnetic structures which we have determined for Rb_2MnF_4 and Rb_2FeF_4 in Sec. IV.

C. Crystal Field and Spin Hamiltonians

1. K_2NiF_4

The crystal-field splittings and ground-state wave functions for Ni^{++} in K_2NiF_4 have been discussed in some detail by Lines.[4] The nickel ground state to a good approximation may be schematically represented as

$$|e^2\,{}^3A_2\rangle-\frac{\sqrt{2}\zeta}{\Delta}|t_2e\,{}^3T_2\rangle-\frac{\zeta}{\Delta'}|t_2e\,{}^1T_2\rangle, \qquad (1)$$

where ζ is the spin-orbit coupling constant ≈ 500 cm^{-1}, Δ, the splitting of the first excited state, equals 7500 cm^{-1}, and $\Delta'=21\,050$ cm^{-1}.[9] Thus the Ni^{++} ion to a good approximation is an orbital singlet with effective $S=1$, and, as is well known, this considerably simplifies the form of the spin Hamiltonian. The wave function (1) is consistent with the g value measured by Birgeneau *et al.*[22] $g_{\parallel}=2.22\pm0.06$.

The spin Hamiltonian in K_2NiF_4 has also been discussed by Lines.[4] He writes

$$\mathcal{H}=\sum_i\sum_{j<i}J_{nn}\mathbf{S}_i\cdot\mathbf{S}_j-\sum_i(g_z\mu_BHS_{zi})+\mathcal{H}_{\text{anis}}+\mathcal{H}_{\text{distant neighbor}}, \qquad (2)$$

where it is assumed that the first term is dominant. Values for J_{nn} have been deduced by Lines[4] and by Maarschall *et al.*[8] from the measured bulk properties; they find $J_{nn}=100\pm10$°K. [See note added in proof.] Information about $\mathcal{H}_{\text{anis}}$ may be deduced from antiferromagnetic resonance; Birgeneau *et al.*[22] find a single magnetic dipole active mode at 27.6°K. This then corresponds to an anisotropy field of $g\mu_BH_A=1.1$°K; this anisotropy field probably contains comparable contributions from each of magnetic dipole interaction, anisotropic exchange, and single-ion crystal-field terms of the form DS_z^2. The sign of H_A, of course, is so as to make the spin point along the c axis. We have no information about the in-plane part of $\mathcal{H}_{\text{distant neighbor}}$ although Lines's assumption that it is much less than $\mathcal{H}_{nn}$ seems quite plausible.

The interactions between planes are rather more difficult to estimate. Any superexchange between nnn layers must involve five intervening anions; using the rule of thumb of a factor of (overlap)$^2\sim10^{-2}$ for each additional ligand, this would imply that the nnn plane exchange integral is $\sim10^{-8}J_{nn}$ although this is probably an underestimate. The corresponding dipolar coupling is $\sim3\times10^{-3}$ °K. In either case it is clear that the interactions between nnn layers are at least four orders of magnitude smaller than the intralayer exchange. It would seem therefore that from the point of view of both intraplane and interplane interactions, K_2NiF_4 should approximate well to a [2] pseudo-Heisenberg model, the anisotropy being only 1 part in 400.

2. Rb_2MnF_4

For Mn^{++} in Rb_2MnF_4 the ground state is $|t_2^3e^2\,{}^6A_1\rangle$ with very small admixtures of the higher ${}^4T_1$ levels via the spin-orbit coupling. The interaction Hamiltonian therefore will be identical to (2) with $S=\frac{5}{2}$ except that

[17] V. Scatturin, L. Corliss, N. Elliott, and J. Hastings, Acta Cryst. **14**, 19 (1961).
[18] E. Legrande and R. Plumier, Phys. Status Solidi **2**, 317 (1962).
[19] H. L. Davis and A. Narath, Phys. Rev. **134**, A433 (1964).
[20] A. Narath and H. L. Davis, Phys. Rev. **137**, A163 (1965).
[21] D. E. Cox, G. Shirane, R. J. Birgeneau, and J. B. MacChesney, Phys. Rev. **188**, 930 (1969).
[22] R. J. Birgeneau, F. De Rosa, and H. J. Guggenheim, Solid State Commun. **8**, 13 (1970).

$\mathcal{H}_{\text{anis}}$ should be almost completely dipolar in origin. Values for J_{nn} have been deduced by Lines[4] and by Breed[10]; they find, respectively, $J_{nn}=6.9\pm0.4$°K and $J_{nn}=6.7\pm0.3$°K, so that a mean of 6.8 ± 0.4°K seems reasonable. The anisotropy energy may be deduced from the spin-flop field of 50.8 kG as measured by Breed. Using this value, one finds $g\mu_B H_{\text{anis}}=0.34$°K compared with the calculated dipolar value of 0.33°K. The assumption that $\mathcal{H}_{\text{anis}}$ is predominantly dipolar in origin, therefore, seems to be a very good one. Breed also has measured the susceptibility of Rb_2MnF_4 and finds an ordering temperature of 38.5°K. In addition, the susceptibility measurements indicate that in the ordered phase the spins point along the tetragonal axis. It seems, therefore, that Rb_2MnF_4 should be closely analogous to K_2NiF_4 in its magnetic properties although the increased anisotropy $H_a/H_e\sim1/200$ in Rb_2MnF_4 versus 1/400 in K_2NiF_4 may have some effect.

3. Rb_2FeF_4

A discussion of the crystal-field effects and associated spin Hamiltonian for Fe^{++} in Rb_2FeF_4 is rather difficult due to the limited amount of available experimental information. At the present time the only quantitative results are Mössbauer effect and bulk susceptibility measurements.[12] Both measurements indicate a transition to LRO between 50 and 60°K, although the Mössbauer spectra were rather complicated and indeed, according to the investigators, seemed to imply a spread in T_N of ~5°K. The susceptibility measurements indicate that in the ordered phase the spins lie in the plane, in contrast to K_2NiF_4 and Rb_2MnF_4 where the spins are thought to point perpendicular to the planes. The Mössbauer spectra also indicate that in the ordered phase there is a small distortion of magnetostrictive origin which lowers the square symmetry in the plane.

Because of the lack of spectroscopic data a precise crystal-field theory for the Fe^{++} ion in Rb_2FeF_4 is not possible. Nevertheless, it is possible to make a reasonable conjecture.[23] The most plausible explanation of the existing data, including our own, is one in which the Fe^{++} ground state is described by an "effective spin $S=2$" but with a moment which may have significant orbital content. The nearest excited states above the ground manifold are sufficiently far away that they will not be important in the temperature range of interest here. The effective spin Hamiltonian therefore may be written in the same way as Eq. (2) for Ni^{++} but with several additional complications. First, the exchange interaction may have significant anisotropic bilinear, biquadratic, and higher-order terms.[24] Second, the single-ion anisotropy terms in the effective spin Hamiltonian must be written

$$\mathcal{H}_{CF}(\text{eff})_i=B_2^0O_2^0(i)+B_4^0O_4^0(i)+B_4^4O_4^4(i), \quad (3)$$

where the O_n^m are the usual Stevens operator equivalents.[25] In Eq. (3) the quadratic term is dominant and $B_2^0>0$ is that the $S_z=0$ state lies lowest.

This gives rise to a rather interesting situation. Although the system has a large axial anisotropy, since the effect of it is to throw the spins into the plane, the system still will not be able to order in two dimensions. (This follows from Mermin and Wagner's exact proof[3] but may also be readily seen by a consideration of the spin waves in this configuration.) The establishment of LRO must then rest on the anisotropy terms within the plane, that is, either $B_4^4O_4^4$ in (3) or else biquadratic exchange; both are likely to be relatively small.

The nn isotropic exchange, J_{nn} in (2) may be estimated from $T_{\chi_{\max}}$, the temperature at which the susceptibility reaches its maximum value, using Lines's formula[26]

$$KT_{\chi_{\max}}/J_{nn}=1.12S(S+1)+0.10. \quad (4)$$

From Wertheim *et al.*'s value[12] of $T_{\chi_{\max}}=90$°K one finds $J_{nn}=13$°K. Unfortunately, no experimental information is available to enable one to estimate the anisotropy present. It is clear, however, that Rb_2FeF_4 should present an interesting contrast to K_2NiF_4 and Rb_2MnF_4.

III. THEORY

A. Neutron Scattering Cross Section

Defining the neutron energy and momentum loss, respectively,[27] as

$$\hbar\omega=E-E'=(\hbar^2/2m_0)(k^2-k'^2), \quad \hbar\mathbf{Q}=\hbar(\mathbf{k}-\mathbf{k}'), \quad (5)$$

the cross section to unpolarized neutrons of N localized spins is

$$\frac{\partial^2\sigma}{\partial\Omega'\,\partial E'}=A(\mathbf{k},\mathbf{k}')\sum_{\alpha\beta}(\delta_{\alpha\beta}-\hat{Q}_\alpha\hat{Q}_\beta)\mathcal{S}^{\alpha\beta}(\mathbf{Q},\omega), \quad (6)$$

where

$$A(\mathbf{k},\mathbf{k}')=(N/\hbar)(r_0\gamma)^2(k'/k)|f(\mathbf{Q})|^2, \quad (7)$$

$r_0=e^2/mc^2$, $f(\mathbf{Q})$ is the neutron scattering form factor and

$$\mathcal{S}^{\alpha\beta}(\mathbf{Q},\omega)=\frac{1}{2\pi}\int_{-\infty}^{\infty}e^{i(\mathbf{Q}\cdot\mathbf{r}-\omega t)}\sum_{\mathbf{r}}\langle S_0^\alpha(0)S_{\mathbf{r}}^\beta(t)\rangle dt, \quad (8)$$

[23] This conjecture follows from the fact that (a) the spins lie in the plane, (b) the electric field gradient at the nucleus is only weakly temperature-dependent, (c) the measured moment is 4–5 μ_B. See J. S. Griffiths, *The Theory of Transition Metal Ions* (Cambridge University Press, New York, 1961), p. 355–360.

[24] R. J. Birgeneau, M. T. Hutchings, J. M. Baker, and J. D. Riley, J. Appl. Phys. **40**, 1070 (1969).

[25] M. T. Hutchings, in *Solid State Physics*, edited by F. Seitz and D. Turnbull (Academic Press Inc., New York, 1964), Vol. 16, p. 227.

[26] M. E. Lines, J. Phys. Chem. Solids **31**, 101 (1970).

[27] For a review see W. Marshall and R. Lowde, Rept. Progr. Phys. **31**, 705 (1968).

that is, the scattering cross section is directly proportional to the space-time Fourier transform of the time-dependent two-spin correlation function.

In general, $\mathcal{S}^{\alpha\beta}(\mathbf{Q},\omega)$ contains essentially all of the physical information of interest. In this particular discussion we shall be interested in two components of $\mathcal{S}^{\alpha\beta}(\mathbf{Q},\omega)$, the elastic part giving rise to Bragg scattering in the ordered phase and the diffusive part which gives rise to critical scattering. These are given by

$$\left(\frac{d\sigma}{d\Omega'}\right)_{\text{Bragg}} = A(\mathbf{k},\mathbf{k}')\sum_{\alpha\beta}(\delta_{\alpha\beta}-\hat{Q}_\alpha\hat{Q}_\beta)\sum_{\mathbf{r}} e^{i\mathbf{Q}\cdot\mathbf{r}}\langle S_0{}^\alpha\rangle\langle S_\mathbf{r}{}^\beta\rangle \quad (9)$$

and

$$\left(\frac{\partial^2\sigma}{\partial\Omega'\,\partial E'}\right)_{\text{diffuse}} = A(\mathbf{k},\mathbf{k}')\sum_{\alpha\beta}(\delta_{\alpha\beta}-\hat{Q}_\alpha\hat{Q}_\beta) \times\frac{1}{2\pi}\int_{-\infty}^{\infty} e^{i(\mathbf{Q}\cdot\mathbf{r}-\omega t)}\sum_{\mathbf{r}}\langle\delta S_0{}^\alpha(0)\delta S_\mathbf{r}{}^\beta(t)\rangle dt, \quad (10)$$

where

$$\delta S_\mathbf{r}{}^\alpha(t) = S_\mathbf{r}{}^\alpha(t)-\langle S_\mathbf{r}{}^\alpha(t)\rangle. \quad (11)$$

We consider first the Bragg scattering. If the system has LRO in three dimensions then $\sum_\mathbf{r} e^{i\mathbf{Q}\cdot\mathbf{r}}$ in (9) will be nonvanishing only for $\mathbf{Q}$ equal to a reciprocal-lattice (rl) vector of the [3] lattice so that we will see conventional Bragg peaks. However, if the system is ordered solely in two dimensions then only spins $\mathbf{r}$ in the same plane as $\mathbf{O}$ can make a contribution to $\sum_\mathbf{r}$. Thus, the scattering cross section will be independent of Q_z, the component of the momentum $\perp$ to the planes. However, the rl will still be well defined within the planes. Thus in a system which has LRO in only two dimensions we will have rl *rods* rather than *points*, where the rods extend in the direction of disorder. For both [2] and [3] order, Eq. (9) predicts that the scattering cross section will be proportional to the square of the sublattice magnetization.

The diffuse scattering $(\partial^2\Omega/\partial\Omega'\partial E')_{\text{diffuse}}$ is somewhat more difficult to treat. For simplicity we limit ourselves to the quasi-elastic approximation, that is, we assume that in our experiment we are integrating over the energy. In that case, Eq. (10) simplifies to

$$\left(\frac{d\sigma}{d\Omega'}\right)_D = \int dE'\left(\frac{\partial^2\sigma}{\partial\Omega'\,\partial E'}\right)_D = A(\mathbf{k},\mathbf{k}')\frac{kT}{g^2\mu_B{}^2}\sum_{\alpha\beta}(\delta_{\alpha\beta}-\hat{Q}_\alpha\hat{Q}_\beta)\chi^{\alpha\beta}(\mathbf{Q}), \quad (12)$$

where $\chi^{\alpha\beta}(\mathbf{Q})$ is the wave-vector–dependent susceptibility. For a [2] system in the Ornstein-Zernike approximation

$$\chi^{\alpha\beta}(\mathbf{Q}) \propto (\kappa^2+q_x{}^2+q_y{}^2)^{-1}, \quad (13)$$

where κ is the correlation length within the planes and $q_\alpha=\tau_\alpha-Q_\alpha$, where τ is a [2] rl vector. Hence, in a [2] antiferromagnet we anticipate critical scattering about the rl points just as in a (3) system with the notable difference that in the [2] case the critical scattering should be independent of Q_z, that is, one should see critical scattering *ridges*. Such critical scattering may be differentiated from [2] Bragg scattering both by its temperature dependence and by its energy dependence.

B. Application to K_2NiF_4

We now consider the consequences of Sec. III A for K_2NiF_4. The real lattice and the corresponding rl for the [3] structure are shown in Fig. 3. As discussed in Sec. III A, if LRO exists in three dimensions then Bragg scattering will be observed at the magnetic rl points in the usual fashion. However, if LRO exists only in two dimensions and the system is disordered in the third direction then these *Bragg peaks* become extended in the third direction giving rise to *Bragg ridges*, that is $(1,0,0)(1,0,2)\rightarrow(1,0,l)$. In K_2NiF_4 with the crystal oriented such that the [0,1,0] magnetic axis is vertical the Bragg ridges should occur at $(h,0,\cdots)$ where h is odd. For the critical scattering, analogous behavior is expected, that is, we should see either peaks or ridges depending upon whether the correlations are [3] or [2] in nature. The critical scattering will be centered about the corresponding Bragg reciprocal lattice positions. Conceptually, therefore, an experiment to establish the [2] nature of the system is quite straightforward. It consists merely of searching for the existence of a ridge using scans of the sort portrayed in Fig. 3.

IV. EXPERIMENT

The elastic scattering experiments were performed mainly on a double-axis spectrometer at the Brookhaven High-Flux Beam Reactor using neutrons of wavelength (λ) 1.029 Å; 20′ collimation before and after the scattering was employed. The monochromator was a germanium crystal reflecting from (3,1,1) in transmission geometry. This choice of reflection minimized beam contamination from $\lambda/2$ neutrons. The inelastic measurements and some of the elastic measurements for Rb_2FeF_4 were performed on a triple-axis spectrometer using neutrons of wavelength 2.618 Å with 20′ collimation. The K_2NiF_4 crystal used in these experiments was a large single crystal 0.5 cm³ in volume with a mosaic spread (full width at half-maximum) of 0.5 deg. The Rb_2FeF_4 crystal was about 0.7 cm³ in volume with a mosaic spread of 0.15 deg. For Rb_2MnF_4, however, the materials situation at the time of this work was not quite so fortunate. We were unable to obtain a good quality large single crystal and instead were forced to work with two multicrystalline samples. The first of these (sample 1) showed a sharp Bragg peak at each rl point with a mosaic spread of about 0.4 deg but with a broad structureless base nearly 6° wide.

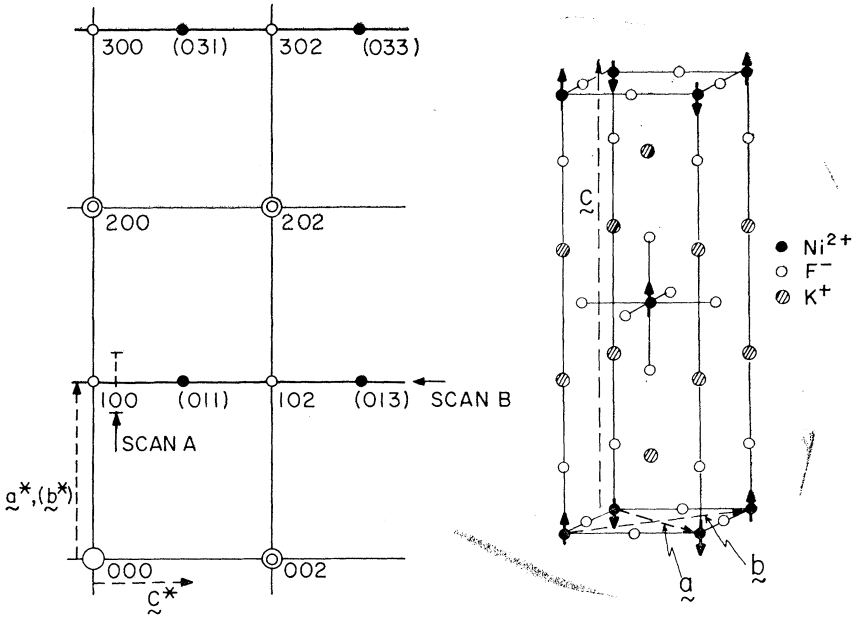

FIG. 3. Right-hand side: Magnetic and chemical structure of K_2NiF_4 with the orthorhombic magnetic axes **a**, **b**, **c** defined. Left-hand side: [0 1 0] and [1 0 0] magnetic zones arising from the two observed domains. The double circles refer to nuclear rl points. The open and filled circles refer to domain-1 and domain-2 magnetic rl points, respectively. The thick lines refer to the magnetic ridge in the two-dimensional phase.

The second sample (sample 2) was composed of several smaller single crystals which gave rise to sharp Bragg peaks distributed over 10° together with a broad base. In the latter case it was possible to cut down the beam so that only a single subcrystal contributed appreciably to the scattering. Our study of Rb_2MnF_4, therefore, was somewhat limited; however, as we shall see later, we were still able to observe interesting effects, the most important of which may in fact have depended on the poor quality of the crystals.

The crystals were each mounted with their [1,1̄,0] chemical axes vertical on aluminum pedestals using Hysol epoxy type 1C; both the pedestal and glue were covered with cadmium. The sample holder was then mounted in a Cryogenics Associate temperature control Dewar. Relative temperatures were found to be reproducible to better than 0.1°K over the entire temperature range studied.

A. Elastic Scattering

1. K_2NiF_4

It is worthwhile recording the actual manner in which these experiments evolved historically. The only studies of K_2NiF_4 which preceded this one were the powder diffraction measurements by Plumier[6] and the susceptibility measurements by Srivastava.[7] In the powder measurements, Plumier observed that the (1,0,0) magnetic peak persisted to about 180°K but with a linewidth which increased with increasing temperature. He explained this by postulating that LRO was established at 180±10°K with a pseudo-LRO being established simultaneously in the third direction but with "stacking faults" between the planes occurring quite frequently. The number of stacking faults was then assumed to decrease with decreasing temperature but still remaining quite large at 4.2°K. The susceptibility, on the other hand, showed no discontinuous behavior at 180°K but instead remained nearly isotropic down to 110°K, at which temperature $\chi_{\parallel}$ and $\chi_{\perp}$ began to separate. Srivastava, therefore, identified this latter temperature as T_N.

The first task in the experiment, therefore, is to locate T_N. To do this, a crystal spectrometer was set up to look at the Bragg scattering from the (1,0,0) magnetic rl point. The temperature was then lowered continuously from 200°K. The results are shown in Fig. 4. As the temperature decreases the scattering intensity increases very slowly but even by 100°K is still two orders of magnitude smaller than the calculated intensity for [3] LRO. However, in cooling from 97.1 to 97.0°K a rather dramatic phase transition occurs. The intensity instantaneously jumps by nearly an order of magnitude and continues to increase rapidly with decreasing temperature. A survey of additional magnetic Bragg peaks shows that [3] LRO has been established with the magnetic structure shown in Fig. 2. The linewidth of the magnetic Bragg peaks is identical to that of the nuclear peaks indicating that the magnetic system has true LRO with no observable effects from stacking faults.

In order to ascertain whether or not there is any critical scattering at all accompanying the abrupt transition to [3] LRO, wide-angle φ scans through (1,0,0) and (0,1,3) were carried out at 97.4°K. The results of these scans are shown in Fig. 5. In both cases the scattering is quite weak; furthermore, it seems to have a totally different character for the two peaks. These single-crystal results, therefore, seem to be at complete variance with Plumier's powder measurements.

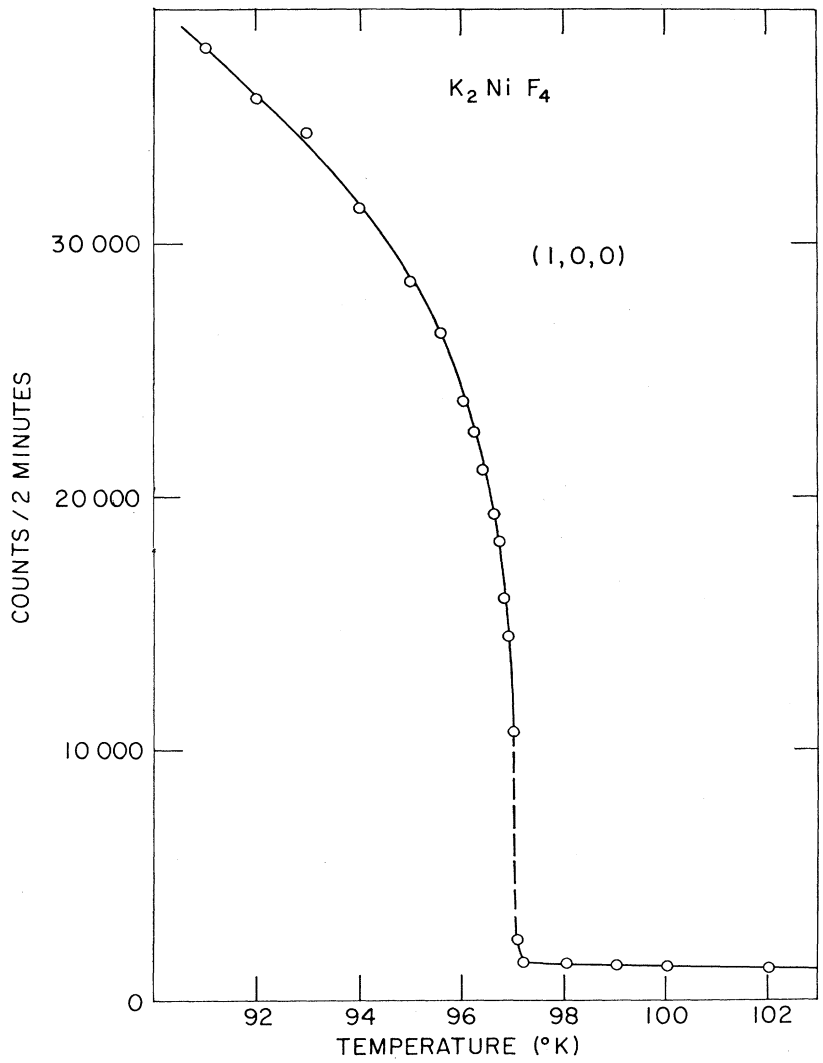

FIG. 4. Intensity variation at the K_2NiF_4 (1,0,0) rl position as a function of temperature in the neighborhood of the phase transition.

In addition, the transition seems to have all of the characteristics normally associated with a *first-order* phase transition—a most unexpected result. Since one source of the apparent discrepancy could be simply the chemistry, it was decided to repeat the powder measurements using our crystals. Powder diffraction patterns were taken at a number of temperatures between 77 and 200°K. We shall discuss these measurements in detail in Sec. IV D. The basic result, however, is that we observe essentially the same temperature evolution of the (1,0,0) magnetic peak as Plumier does.

Any attempt to resolve this apparent paradox immediately leads one to the theoretical discussion given previously in Sec. III and, in particular, to the concept of the "ridge." It is then clear that most features of these preliminary results may be accounted for simply by assuming that $T_N=97.1$°K is the [3] phase-transition temperature and that above 97.1°K the system is [2] in character. To verify this we must establish directly the existence of the ridge. As discussed in Sec. III this can be done easily by carrying out scans of types A and B, as shown in Fig. 3.

The experimental results at 99 and 95°K are given in Fig. 6. From the figure it may be seen that at 99°K the ridge does indeed exist. Scan B along $(1,0,l)$, that is, along the top of the ridge, gives a constant value far above the background. The decrease in intensity at large l is due to geometrical factors.[28] The important feature is that there is no peaking whatsoever about (1,0,0) and (0,1,1) as would occur in a normal [3] system. Scan A along $(h,0,0.25)$, that is, perpendicular to the ridge, shows a sharp peak with a linewidth determined by the instrumental resolution. The lack of concavity in scan B together with the sharpness of scan A shows unambiguously that at 99°K, K_2NiF_4 behaves as a pure two-dimensional antiferromagnet with very long-range correlations within the planes (>1000 Å) and no measurable correlations between the planes.

[28] J. Skalyo, Jr., G. Shirane, and R. J. Birgeneau (unpublished).

We believe that this is the first time that such two-dimensional scattering has been observed in a magnetic system.

The scattering remains essentially identical in form down to 97.2°K. However, in cooling from 97.2 to 97.0°K a rather unusual phase transition is observed. Sharp Bragg *peaks* appear on top of the ridge at the magnetic reciprocal lattice points (1,0,0), (0,1,1), etc. The intensity of the (1,0,0) peak at 97.0°K is about 13% of its value at 4.2°K and, as noted previously, the linewidth is just the mosaic spread of the crystal indicating that true LRO in all three dimensions has been established. The scattering at 95°K is shown in Fig. 6. From the figure it may be seen that at 95°K the ridge has remained essentially identical to that at 99°K except that it has decreased in intensity by about $\frac{1}{3}$. In addition, it has developed sharp peaks at the (1,0,0) and (0,1,1) rl positions. Approximate integration indicates that the intensity in the Bragg peak is just that lost by the ridge.

In order to ascertain the nature of the [2] region above 97.1°K it is necessary to study the evolution of the rod with temperature. A series of scans of types A, B show that the ridge remains well defined up to at least 200°K. The (1,0,0.25) peak intensities together with the (1,0,l) ridge linewidths as a function of temperature are shown in Fig. 7. From the figure it may be seen that the (1,0,l) ridge reaches its limiting intensity and linewidth at T_N. The behavior in the range from 97.2 to 200°K thus seems to be exactly analogous to the critical region in a [3] system except that the temperature scale is greatly expanded. For comparison purposes it is interesting to note that in $KMnF_3$[29] at $T/T_N=1.1$ the correlation range has decreased to 12 Å whereas here at $T/T_N=2$ the range within the planes as estimated from the inverse linewidth is 23 Å. A proper analysis of the linewidth measurements requires further investigation involving precise resolution corrections. Nevertheless, the qualitative observation of the wide temperature range over which there are very long correlations within the planes is really quite remarkable. This is clearly a unique physical property which arises from the [2] nature of the system. It must also be intimately related to the near-Heisenberg form of the interactions since the critical region in the [2] $S=\frac{1}{2}$ *Ising model* is not predicted to be very different from that in [3] systems.[5]

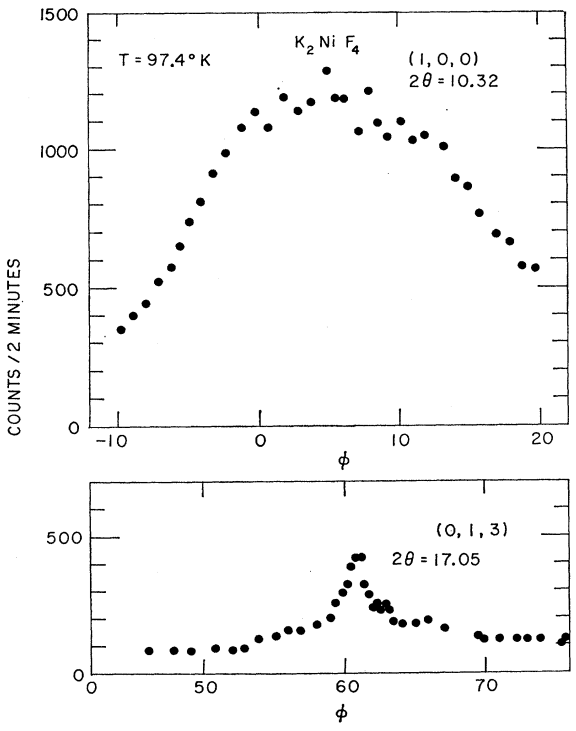

FIG. 5. Wide-angle φ scans ($2\theta_B$ held fixed) through (1,0,0) and (0,1,3) above the phase transition in K_2NiF_4.

TABLE II. Magnetic Bragg peak intensities in Rb_2MnF_4 at 4.3°K.

h k l[a]	I_{expt}[b]	I_{calc}[b]	Normalized[c] ratio
1 0 0	5.13	4.21	0.77
1 0 2	1.98	1.61	0.78
1 0 4	0.50	0.33	0.97
1 0 6	0.15	0.07	1.3
3 0 0	0.73	0.42	1.09
3 0 4	0.32	0.18	1.1
0 1 1	3.54	3.16	0.71
0 1 3	1.14	0.73	0.99
0 1 5	0.30	0.15	1.3
1 0 $\frac{1}{2}$	7.24	3.90	0.76
1 0 $\frac{3}{2}$	4.17	2.34	0.73
1 0 $\frac{5}{2}$	2.24	1.09	0.84
1 0 $\frac{7}{2}$	1.26	0.49	1.05
1 0 $\frac{9}{2}$	0.63	0.22	1.2
3 0 $\frac{1}{2}$	1.46	0.42	1.42

[a] Indexed on the magnetic cell shown in Fig. 3.
[b] These are both in arbitrary units; for the calculated intensities it is assumed that the spin is pointing along the c axis for both phases.
[c] The ratio is normalized separately for the two different types of peaks; the large scatter in the ratio is probably due to poor quality of the crystal.

Let us now consider the behavior for $T<T_N$. First, as shown in Fig. 7 the ridge decreases extremely rapidly in intensity with decreasing temperature. Concomitantly, the (1,0,0) peak intensity increases equally rapidly with decreasing temperature and indeed, continues to increase down to 4.2°K; this is in contrast to normal [3] systems where the magnetic Bragg scattering intensity saturates quite quickly. We shall discuss this behavior in more detail in Sec. IV B. θ, 2θ scans through (1,0,0) at 95°K show no evidence at all for [3] critical scattering. Thus the diffuse scattering below T_N retains the form of a ridge. In the immediate neighborhood of T_N, at least, this diffuse scattering may be thought of as the $T<T_N$ counterpart of the [2] critical scattering observed above T_N.

In Sec. V, we shall propose a model which we hope will give a unified picture of the elastic scattering for all T.

[29] M. J. Cooper and R. Nathans, J. Appl. Phys. **37**, 1041 (1966).

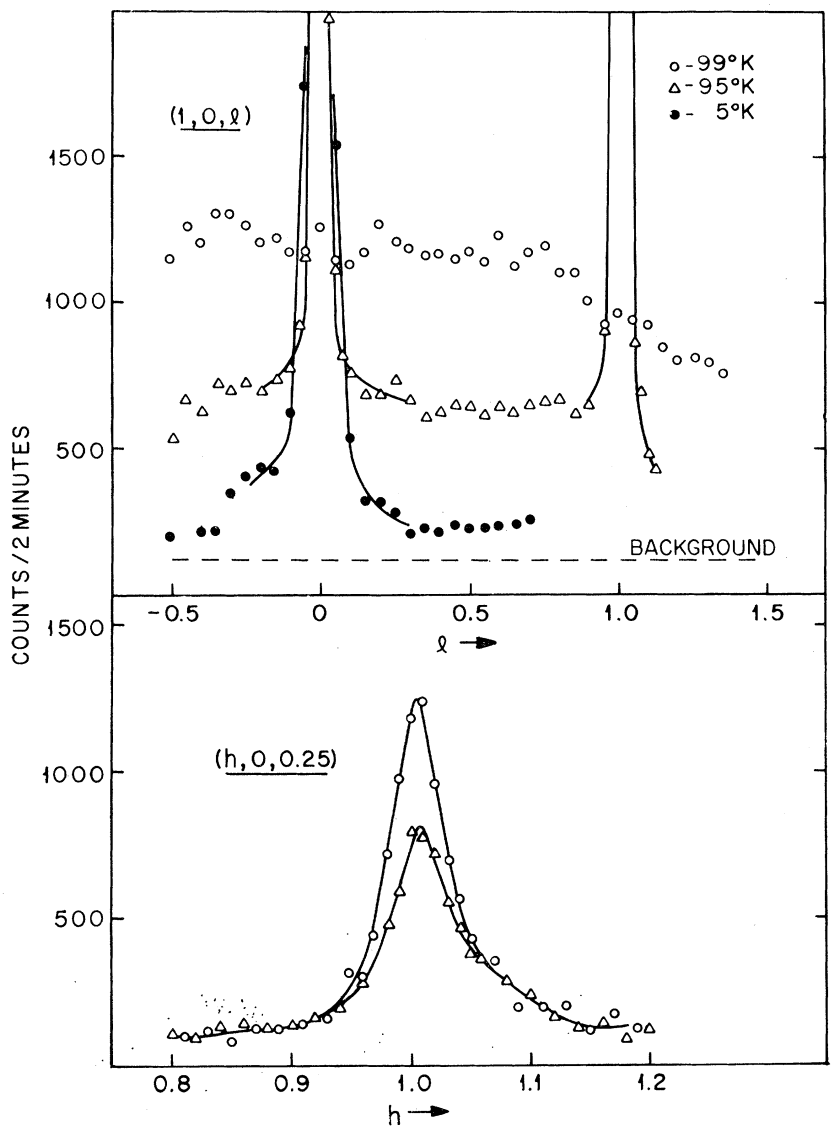

FIG. 6. The upper set of curves corresponds to scan *B* along the top of the ridge as shown in Fig. 3; the lower set of curves corresponds to scan *A* across the ridge in K_2NiF_4.

2. Rb_2MnF_4

In Sec. II C, it was pointed out that on the basis of the existing data, it seems likely that the behavior of Rb_2MnF_4 will be rather similar to that of K_2NiF_4. To begin our study of Rb_2MnF_4 we must then first determine the magnetic structure. Sample 1, which was oriented with a $[1,\bar{1},0]$ chemical axis vertical, was cooled to 4.3°K, well below the ordering temperature. A series of φ scans were then carried out through magnetic rl points appropriate to both the K_2NiF_4 and Ca_2MnO_4 magnetic structures. In Table II we list the peak intensities observed at a series of these points. From the table it may be seen that, quite surprisingly, magnetic scattering is observed at *both* types of rl points. As a check φ scans were then carried out through a large number of other possible rl points; it was found in all cases that scattering is observed only at positions which can be indexed on the nuclear cell or on either the K_2NiF_4 on Ca_2MnO_4 magnetic cells. Furthermore, the relative intensities of the K_2NiF_4-type peaks and Ca_2MnO_4-type peaks are internally consistent if the spin direction is taken as the *c* axis for both phases; however, the intensities of the two phases bear no obvious relationship to each other. The simplest explanation of the observed magnetic peaks is that both phases are present simultaneously in the crystal. Indeed, it is extremely difficult to construct any other model which can explain both the spin direction (the susceptibility results[10] also gave the *c* axis as the spin direction in the ordered phase) and the relative intensities. As a consistency check the magnetic Bragg scattering was also studied at 4.3°K in sample 2. In this case the scattering was essentially identical to that observed in sample 1 except that the relative intensities of the Ca_2MnO_4-type peaks to the K_2NiF_4-type peaks

were about 4:1 as opposed to 1.5 to 1 in sample 1. This change in relative intensities can only be explained using the two-phase model. As we shall see later, this is really a very important result. Although the perovskite-type antiferromagnetic ordering within the MnF_2 planes is retained, apparently the coupling between the nnn planes is so weak in Rb_2MnF_4 that the two phases are very nearly energetically equivalent, so that local microscopic phenomena (e.g., impurities, dislocations) determine which way each domain actually orders. This is, of course, quite reminiscent of Plumier's suggestion of *stacking faults*.[6] However, in this case, the peak linewidths for both phases are just the mosaic spread of the crystal so that the domains must be at least hundreds of Angstroms in length. We shall discuss the behavior of the sublattice magnetization in Sec. IV B. We note here only that both phases show a very sharp phase transition as the temperature is increased from 38.3 to 38.4°K. Therefore, we take $T_N = 38.4$°K for both phases.

The form of the scattering above the phase transition is given in Fig. 8. Once again we see that the critical scattering has the form of a ridge. Scan B along $(1,0,l)$, that is, along the top of the ridge, gives a constant value far above the background. Scan A, along $(h,0,0)$, that is, perpendicular to the ridge, gives a sharp Lorentzian-like peak. At 38.8°K the width is close to being resolution-limited, implying that at that temperature the correlation length is $\gtrsim 1000$ Å, but by 41°K the intrinsic width has begun to manifest itself clearly. A detailed study of the temperature dependence of the ridge is not particularly fruitful in this case because of the poor quality of our crystals. However, a rough survey shows that the general behavior of the ridge in Rb_2MnF_4 is quite similar to that in K_2NiF_4. In particular, there are still appreciable correlations up to nearly $2T_N$. The behavior for $T<T_N$ is again similar to that in K_2NiF_4 except, of course, for the additional complications of the two phases.

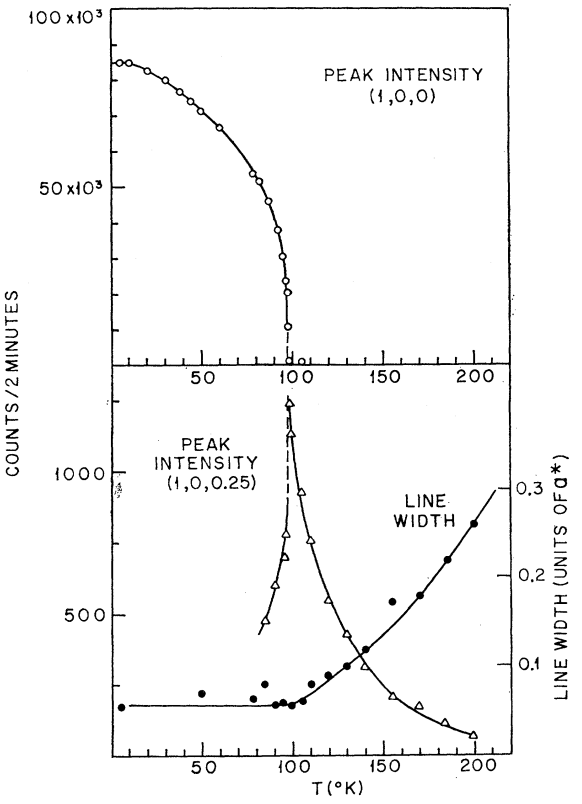

FIG. 7. Scattering intensity in K_2NiF_4 at peak intensity (1,0,0) top, and (1,0,0.25) bottom, together with the linewidth in rl units (full width at half-maximum) for scan A in Fig. 3 as a function of temperature.

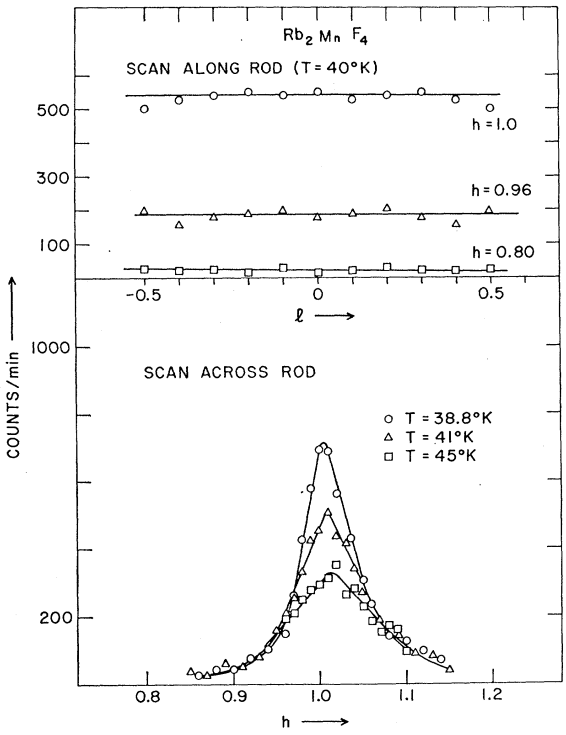

FIG. 8. The upper set of curves corresponds to scans along the top and side of the ridge in Rb_2MnF_4; the lower set of curves corresponds to scans across the ridge.

3. Rb_2FeF_4

As discussed in Sec. II, the magnetic behavior of Rb_2FeF_4 is expected to be somewhat more complicated than that of either K_2NiF_4 or Rb_2MnF_4. We must begin our study of this material by establishing its magnetic structure. The crystal, which was again oriented such that the [0,1,0] and [1,0,0] magnetic zones could be studied, was accordingly cooled to 4.3°K and a series of possible magnetic peaks were surveyed. In all cases it was found that scattering is observed only at positions which can be indexed on the K_2NiF_4 magnetic cell. The relative intensities of the peaks show that the spin is oriented directly along the **b** axis as defined in Fig. 3, with no indication of any canting. Observed and calculated intensities for a

TABLE III. Magnetic Bragg peak intensities in Rb_2FeF_4 at 4.3°K.

h k l	Observed intensity[a]	Calculated intensity[a]	Normalized ratio[b]
1 0 0	899.6	57.1	1.10
1 0 2	536.6	39.0	0.96
1 0 4	268.5	19.2	0.97
1 0 6	125.1	8.7	1.00
1 0 8	50.3	3.7	0.94
3 0 0	120.2	7.0	1.19
0 1 1	182.2	8.11	0.87
0 1 3	336.4	17.44	1.00
0 1 5	207.8	10.73	1.00
0 1 7	99.8	5.18	1.00
0 1 9	37.9	2.23	1.15

[a] These are each in arbitrary units; for the calculated intensities it is assumed that the spin is pointing along the b axis.
[b] The ratio is normalized separately for the two domains.

number of peaks are given in Table III. In general, the agreement is rather good. The calculated intensities are based on the form factor for Fe^{++} given by Watson and Freeman.[30]

The fact that the spins are oriented along an in-plane axis which is unique with respect to the [3] order is both a surprising and very interesting result. It should be noted that Wertheim *et al.*[12] in their Mössbauer study of Rb_2FeF_4 showed that there is an in-plane crystallographic distortion below T_N and they then went on to suggest that this might destroy the condition for the cancellation of interplane interactions. Apparently this is precisely what occurs. The spins always lie in the ferromagnetic (1,0,0) sheets.

The behavior of the (1,0,0) peak intensity in the region of the phase transition is shown in Fig. 9. If we compare this with the corresponding curve for K_2NiF_4 given in Fig. 4 we see that the behavior of Rb_2FeF_4 is quite different. Rather than the sharp quasidiscontinuous behavior characterizing the K_2NiF_4 and Rb_2MnF_4 phase transitions, Rb_2FeF_4 exhibits a smooth continuous change in Bragg peak intensity. The phase transition, therefore, seems to be spread over several degrees. This, of course, is exactly what one sees in normal [3] systems such as $RbMnF_3$ because of the presence of [3] *critical scattering*; that is, the scattering observed at a magnetic rl point is composed both of Bragg scattering, which goes to 0 at T_N and critical scattering which peaks at T_N; hence, the net observed scattering shows no sharp behavior at the phase transition.

In order to establish the nature of the scattering surface around T_N, a series of scans along (1,0,l) and (h,0,0) were carried out. Some of these are shown in Fig. 10. First, we note that at 59.1°K the scattering cross section has the form of a rod. Scans across the rod at (h,0,0) and (h,0,0.5) show that it is Lorentzian-like and essentially independent of position along q_z, the momentum component perpendicular to the planes. By 57.2°K the rod has increased in intensity and, in addition, there is a very weak [3] peak at (1,0,0). In lowering the temperature to 56.8°K the main change is that the [3] peak increases somewhat in intensity. The intensity of the (1,0,0) peak at 56.8°K is approximately two orders of magnitude weaker than the corresponding Bragg peak at 4.2°K. The (1,0,0) peak then continues to increase with decreasing temperature in the manner shown in Fig. 9. The corresponding temperature variation of the rod is also given in Fig. 9. The rod itself shows entirely conventional behavior. The intensity rises to a maximum at 56.3±0.2°K and then falls off with decreasing temperature. Over the entire temperature range shown the scattering is resolution-limited, so that the intensity does not actually diverge as anticipated at a phase transition for a δ-function probe. Nevertheless, the peak in the rod intensity seems sufficiently well defined to justify the identification of (56.3±0.2)°K as the Néel temperature. A number of careful scans through (1,0,0) were also carried out at temperatures in the neighborhood of 56.3°K. In all cases it was found that the linewidth was just that of the resolution ellipse.

The temperature variation of the rod intensity and linewidth over a wide range of temperatures is shown in Fig. 11. A comparison of this with the corresponding results for K_2NiF_4 given in Fig. 6 shows that the two are strikingly similar. The linewidth is slightly larger at a given reduced temperature for Rb_2FeF_4 but there is no real qualitative difference. Thus, although the [3] aspects show some differences in the two systems the [2] properties are virtually identical.

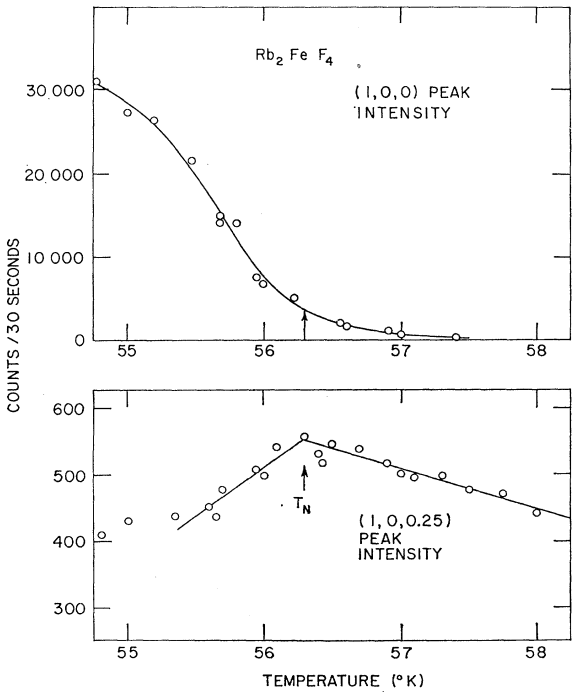

FIG. 9. Intensity variation in Rb_2FeF_4 at the (1,0,0) rl position (top) and (1,0,0.25) ridge position (bottom) as a function of temperature in the immediate neighborhood of the phase transition.

[30] R. E. Watson and A. J. Freeman, Acta Cryst. 14, 27 (1961).

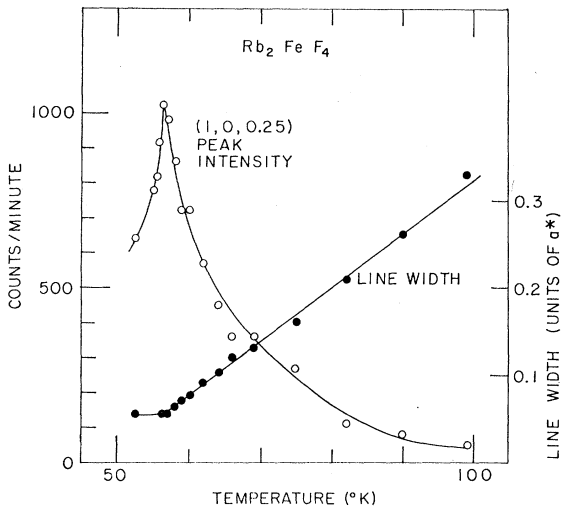

FIG. 10. Temperature variation of the Rb_2FeF_4 ridge peak intensity and linewidth.

B. Sublattice Magnetization Measurements

In Sec. III A, we noted that the magnetic Bragg scattering intensity in an antiferromagnet is proportional to the square of the sublattice magnetization. In the critical region it is expected that the sublattice magnetization will vary like

$$M(T)/M(0)=B(1-T/T_N)^{\beta}, \qquad (14)$$

where both β and B may be calculated from theory in certain cases.[5] In three dimensions, typically $\beta\simeq\frac{1}{3}$ and $B\simeq 1.2$–1.6 whereas in [2] Ising model $\beta=\frac{1}{8}$ and $B\simeq 1.2$ and 1.7.[31] For the [2] square net B is calculated to be 1.2224.[5] Thus in the critical region one expects

$$I_{\text{Bragg}}(T)/I_{\text{Bragg}}(0)=B^2(1-T/T_N)^{2\beta}, \qquad (15)$$

and therefore the critical exponent β and the factor B may easily be determined simply by measuring the intensity of a Bragg superlattice line as a function of temperature.

There are several possible difficulties which may arise in such an experiment. First, in writing Eq. (9) we have omitted the effects of the zero-point and thermally induced vibrations of the atoms, that is, the Debye-Waller factor. This will introduce an additional temperature dependence superimposed upon that given by Eq. (15). However, these effects are small and in fact in the temperature regime which we are interested in here the Debye-Waller factor is determined almost completely by the zero-point vibrations. Hence, we can ignore this effect. Second, as noted in Sec. IV A, the scattering at a magnetic rl point includes not only the Bragg scattering but also the diffuse critical scattering. In conventional [3] systems this can present some difficulty for temperatures very near T_N. However, in K_2NiF_4 and Rb_2MnF_4 we are in a unique position. The Bragg scattering occurs only at a rl points corresponding to the [3] lattice. On the other hand, as we have seen in Sec. IV A, the critical scattering is entirely [2] in form both above and below the phase transition. Thus one can simply measure the critical scattering contribution at a point along the *ridge* away from the rl *point* and then subtract it off directly. The final complicating factor is extinction. Since the effects of extinction increase with increasing peak intensity, they may radically alter the I-versus-T relationship. This may be corrected for if the form of the extinction is known exactly. However, ideally one hopes that no extinction is present. There are two straightforward means of checking this effect. The first is to measure a series of nuclear Bragg peaks to see if there is any discrepancy between theory and experiment which shows a systematic variation with intensity. The second is simply to measure the I-versus-T relationship for magnetic Bragg peaks of quite different intensities. There are several other more trivial difficulties which can effect I-versus-T measurements but in our case none of these were found to be important so we shall not discuss them here.

1. K_2NiF_4

We have already briefly discussed the sublattice magnetization measurements for K_2NiF_4 in Sec. IV A. Before interpreting the results in terms of Eq. (15) we

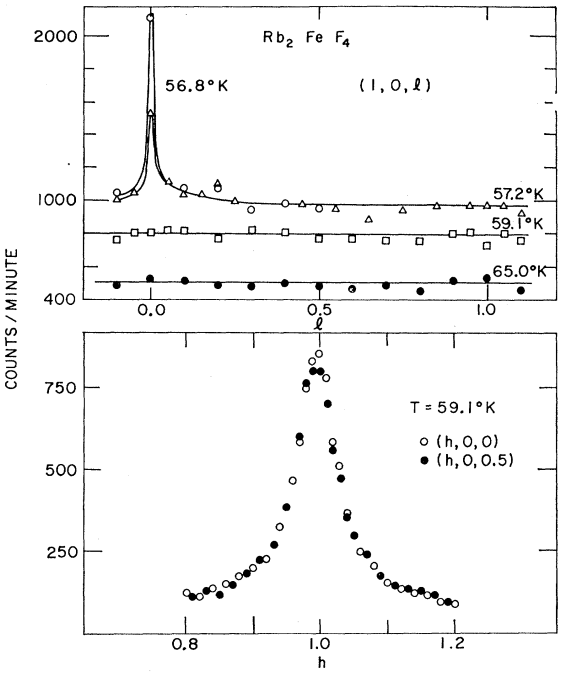

FIG. 11. The upper set of curves corresponds to scan B along the top of the ridge in Rb_2FeF_4 as shown in Fig. 3. Note that the zero is misset. The lower set of curves corresponds to scan A across the ridge at two different positions.

[31] For a review of the experimental situation see P. Heller, Rept. Progr. Phys. 30, 731 (1967).

TABLE IV. Fit to K_2NiF_4 nuclear Bragg intensities at 4.2°K.

h k l	I_{expt}	I_{calc}
0 0 4	3.39	2.64
1 1 14	3.57	3.29
1 1 16	3.70	4.25
3 3 6	3.90	3.73
3 3 4	4.44	4.44
3 3 10	5.40	6.04
3 3 0	6.01	6.02
2 2 2	6.88	6.39
1 1 6	7.60	6.73
1 1 10	8.59	8.28
1 1 4	10.93	9.56
2 2 12	13.61	13.76
2 2 8	14.49	14.88
1 1 0	15.34	16.58
0 0 12	16.89	16.40
2 2 14	19.08	21.33
0 0 8	21.97	21.76
0 0 14	23.09	23.85

$Z_F=0.152\pm0.002$
$Z_K=0.352\pm0.003$
$B=0.15\ \pm0.07$
$R=\sum|I_{expt}-I_{calc}|/\sum I_{calc}=0.056$

must first investigate the effects of extinction. Accordingly, the integrated intensities of a number of nuclear Bragg peaks were determined via φ scans. These intensities were then fitted in the usual manner using the nuclear scattering lengths b(potassium)$=0.37$, b(nickel)$=1.03$, b(flourine)$=0.55$ in units of 10^{-12} cm [32] and allowing a scale factor, an isotropic temperature factor, and the positional parameters for the potassium and flourine in the $(0,0,z_K)$, $(0,0,z_F)$ positions to vary as free parameters. The results are given in Table IV. From the table it may be seen that the fit is quite good. The R factor is 0.056. Most importantly, there is no apparent variation of the quality of the fit with intensity at all thus showing that extinction effects are negligible. The positional parameters are found to be $z_F=0.152\pm0.002$, $z_K=0.352\pm0.003$ compared with 0.151, 0.352 found by Balz and Pleith[16] in their x-ray investigation. The agreement is again excellent. It should be noted that our value of z_F gives the out-of-plane flourine distance as 1.982 ± 0.039 Å compared with 1.997 Å for the in-plane flourines so that the errors allow for both positive and negative distortions of the flourine octahedron. Balz and Pleith have a much larger R factor so that their errors must be correspondingly larger.

The variation of the (1,0,0) Bragg peak intensity as a function of temperature is shown in Figs. 4 and 7. Again we must emphasize that this is the intensity of a [3] peak not a rod. The data analysis is quite straightforward. The background is first subtracted off and the data then reduced to the form $M(T)/M(4.2°K)$.[33] This may then be fitted to a power law for various ranges of reduced temperature. Quite remarkably, these calculations show that for K_2NiF_4, the data can be fitted satisfactorily *at all temperatures* to a simple power law of the form

$$M(T)/M(4.2°K)=1.02(1-T/97.05)^{0.14}. \quad (16)$$

This fit holds over the range $\sim10^{-3}<1-T/97.05<0.9$. The actual data are shown in Fig. 12. If we instead limit the data to the more usual "critical region" we find a somewhat improved fit with

$$M(T)/M(4.2°K)=0.98(1-T/97.04)^{0.14}. \quad (17)$$

This holds for $\sim10^{-3}<1-T/97.04<6\times10^{-2}$. The parameters are tabulated in Table V together with the associated errors. From the table we see that to within the error, there is no difference between the two sets of parameters.

Corresponding results for the [3] antiferromagnet MnF_2 and the exact result for [2] $S=\frac{1}{2}$ Ising model are also shown in Fig. 12. Both differ appreciably from our results for K_2NiF_4 although the β appropriate to K_2NiF_4 is in fact quite close to the $\frac{1}{8}$ characterizing the [2] Ising model. The principle difference is that for the [2] Ising model a power law is no longer a good approximation for $1-T/T_N>\sim10^{-1}$.

The results for $1-T/T_N>10^{-1}$ are shown in more detail in Fig. 13. The solid line corresponds to the power law $1.02\ (1-T/97.05)^{0.14}$, whereas the broken line is the magnetization calculated using noninteracting [2] spin-wave theory. This spin-wave curve was kindly calculated for us by Lines. The theory uses the spin-Hamiltonian parameters given in Sec. II A and hence contains *no adjustable parameters*. The agreement

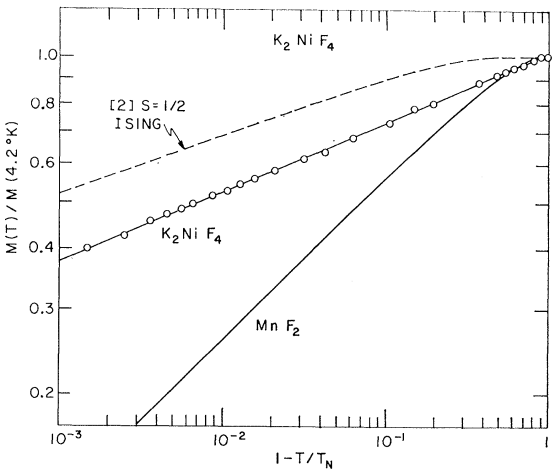

FIG. 12. Reduced sublattice magnetization versus reduced temperature for K_2NiF_4, MnF_2 and the [2] $S=\frac{1}{2}$ Ising model. The MnF_2 results are taken from P. Heller, [Phys. Rev. **146**, 403 (1965)]; the [2] $S=\frac{1}{2}$ Ising curve is Onsager's exact result $M_0(T)=(1-\sinh^{-4}\ 2J/kT)^{1/8}$ [L. Onsager, Nuova Cimento Suppl. **6**, 261 (1949)]. We have implicitly assumed $M(4.2)=1$ in this diagram. The solid line through the K_2NiF_4 data is the best fit to a simple power law at all temperatures as discussed in the text.

[32] The Neutron Diffraction Commission, Acta Cryst. **A25**, 391 (1969).

[33] Strictly speaking, the function of interest is $M(T)/M(0)$. However, for all cases considered here this will be identical to $M(T)/M(4.2°K)$ within the errors quoted.

TABLE V. K_2NiF_4 sublattice magnetization parameters.

	$\sim 10^{-3} < 1 - T/T_N < 0.9$	$\sim 10^{-3} < 1 - T/T_N < 6 \times 10^{-2}$
B	1.02±0.01	0.98±0.03
T_N	97.05±0.009	97.04±0.07
β	0.14±0.01	0.14±0.01

between spin-wave theory and experiment for temperatures up to 80% of T_N is excellent. This is by far the widest range over which noninteracting spin-wave theory has been found to hold in any system. Least-squares fits were also carried out for the "low-temperature" data, $1 - T/T_N > 2 \times 10^{-1}$, with T_N fixed at 97.05 and B and β allowed to vary as free parameters. The fit was found to give identical results to that for all T. It would appear, therefore, that by a remarkable coincidence the power law which best fits the spin-wave region is in fact precisely that which characterizes the critical regime. We shall postpone more detailed discussion of these results to Sec. V.

Note added in proof. Since this paper was accepted for publication, measurements of the spin-wave spectra in K_2NiF_4 have been carried out by Skalyo, Shirane, Birgeneau, and Guggenheim [Phys. Rev. Letters **23**, 1394 (1969)]. They find $J_{nn} = 78.1$ cm^{-1}, $g\mu_B H_A = 0.59$ cm^{-1} which differ slightly from the values given in Sec. II A. Calculations with these parameters show that the agreement between spin-wave theory and experiment begins to break down at $\sim \frac{1}{2} T_N$. Our low-temperature sublattice magnetization measurements have also recently been confirmed by high-precision NMR measurements [DeWijn, Walstedt, Walker, and Guggenheim, Bull. Am. Phys. Soc. **15**, 338 (1970)].

The final piece of information which one can derive from the measurements is the static magnetic moment itself. The theory appropriate to this type of neutron measurement has been discussed in some detail by Hubbard and Marshall[34] and the reader is referred to this paper for the details; we present here only the final results. The static moment per unit cell should be reduced from its value in the paramagnetic state both by covalency and by zero-point spin deviation. Hubbard and Marshall have shown that within the MO-LCAO approximation in antiferromagnetic $KNiF_3$ the effective moment is reduced by covalency by $3(A_s^2 + A_\sigma^2)$ where A_s, A_σ are the usual covalency parameters. For K_2NiF_4 the theory is somewhat more complicated but for scattering with $(\sin\theta)/\lambda \geq 0.1$ it should reduce to that of $KNiF_3$. Using the values of the transferred hyperfine-interaction tensor as measured by Maarschall *et al.*[8] we find that for K_2NiF_4, $3(A_s^2 + A_\sigma^2)_{av} = 0.13$ where the average is performed over the two types of fluorine sites. The zero-point contribution to the spin reduction has been calculated by Lines[35] to be 17.5%. Hence, the net reduction due to the two effects should be $1 - 0.825 \times 0.87 = 0.28$. Using the form factor measured for Ni^{++} in NiO [36] and $KNiF_3$ [17] together with the scale factor deduced from the fit to the nuclear peaks we find that all of the magnetic peaks from (1,0,0) through (1,0,6) can be accurately fitted with $\mu = 1.86 \pm 0.1\ \mu_B$. This corresponds to a reduction of 15±5% from the moment of $2.22\mu_B$ as measured by antiferromagnetic resonance. This is significantly smaller than the value of 28% predicted by theory. It is not possible to say, however, whether the error lies in the covalency part or the zero-point spin deviation part of theory, or, in fact, in both. In addition, our application of the theory is somewhat oversimplified. It would, however, be very interesting to resolve this question; explicit theoretical calculations of the covalency effects in antiferromagnetic K_2NiF_4 would be of great value in this regard.

2. Rb_2MnF_4

Measurements of the sublattice magnetization in Rb_2MnF_4 were carried out using the (1,0,$\frac{3}{2}$) aud (1,0,2) peaks in sample 2 and (1,0,0), (1,0,$\frac{1}{2}$), (0,1,1) in sample 1. Neutrons of wavelengths 1.221 and 1.026 Å were employed for samples 2 and 1, respectively. Intensities were determined both by integration and by taking the peak intensity alone with the background being properly removed in all cases. Additional checks for extinction were also made using the (0,1,1), (1,0,2), (0,1,3) peaks in sample 2. Both samples were found to

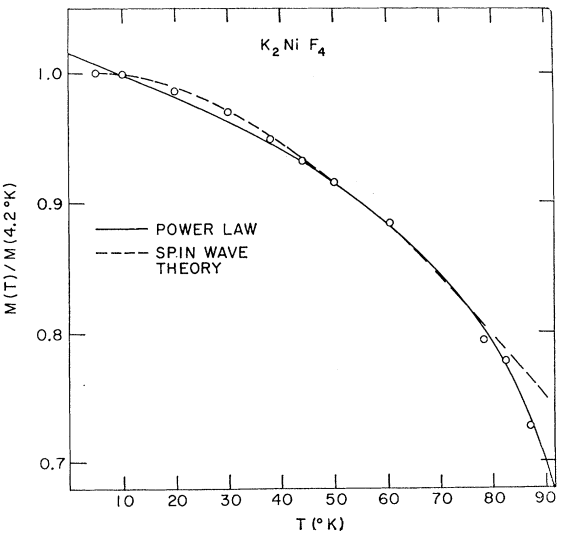

FIG. 13. K_2NiF_4 sublattice magnetization as a function of temperature outside of the critical region. The solid line is the power law shown in Fig. 12; the broken line is the magnetization calculated by Lines using noninteracting spin-wave theory.

[34] J. Hubbard and W. Marshall, Proc. Phys. Soc. (London) **86**, 561 (1965). For more recent theoretical considerations see D. E. Ellis and A. J. Freeman, in Proceedings of the Fifteenth Annual Conference on Magnetism and Magnetic Materials, Philadelphia, 1969, J. Appl. Phys. (to be published).

[35] M. E. Lines (private communication).

[36] H. Alperin, Phys. Rev. Letters **6**, 55 (1961).

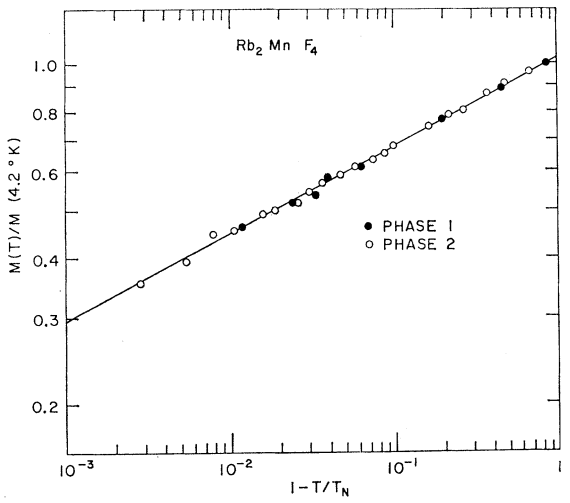

FIG. 14. Reduced sublattice magnetization versus reduced temperature for Rb_2MnF_4 for the two [3] magnetic structures. The solid line is the best fit to the data of a simple power law at all temperatures.

give extinction-free magnetic peaks. In addition, both the integrated intensities and peak intensities gave identical magnetization curves. The principal result of the measurements is that in all cases the experimental sublattice magnetization curves are identical to within experimental errors. First, this means that within the K_2NiF_4 phase (phase I) the two domains have constant relative populations and second, the Ca_2MnO_4 phase (phase II) also has the same M-versus-T relationship.

As noted previously, both K_2NiF_4 and Ca_2MnO_4 have simple square antiferromagnetic-spin arrays within the planes but with nnn planes stacked ferromagnetically in the former case and antiferromagnetically in the latter. We thus have the remarkable result that in Rb_2MnF_4 the sublattice magnetization is independent of the [3] ordering pattern for all temperatures (with temperature control of 0.1°K) and instead apparently depends solely on the [2] magnetic structure. To our knowledge, this is the first time that such behavior has been observed. This sublattice magnetization may now be fitted to an appropriate power law. The results of such a fit to the data are shown in Fig. 14. Once more, it is found that a simple power law accurately describes the magnetization *at all temperatures*. The solid line in the figure corresponds to

$$M(T)/M(4.2°\mathrm{K}) = 1.02(1-T/38.4)^{0.18}. \quad (18)$$

Both B and β are quite close to the corresponding values in K_2NiF_4. If we limit the data to $1-T/T_N<10^{-1}$, we find a somewhat improved fit with

$$M(T)/M(4.2°\mathrm{K}) = 0.96(1-T/38.37)^{0.16}, \quad (19)$$

again quite close to the corresponding law for K_2NiF_4. This holds for $3\times10^{-3}<1-T/38.4<10^{-1}$. The parameters are tabulated in Table VI.

TABLE VI. Rb_2MnF_4 sublattice magnetization parameters.

	Phase II	Phase I	Phase II $(1-T/T_N)<10^{-1}$
B	1.02±0.03	1.02±0.05	0.96±0.06
T_N	38.41±0.07	38.37±0.07	38.37±0.07
β	0.18±0.01	0.18±0.02	0.16±0.02

Lines has also carried out calculations of the sublattice magnetization using noninteracting spin-wave theory with the parameters given in Sec. III, $J_{nn}=6.8$°K, $H_a/H_e=0.005$. A comparison of these spin-wave values with our experimental results shows that although there is qualitative agreement, the temperature scale for the spin-wave curve must be expanded by about 13% to obtain quantitative agreement. This is equivalent to increasing J from 6.8 to ~7.8°K. The agreement is then reasonably good up to about 25°K, that is, 65% of T_N. Our treatment of this is rather rough, however; a more refined application of the theory together with more precise measurements are required to determine the explicit range over which simple spin-wave theory holds. It is interesting to note, nevertheless, that the large value of J_{nn} we seem to require is consistent both with the measured Weiss-θ constant and χ_{II} in the ordered phase[10]; they give $J_{nn}=7.5\pm0.8$°K and 7.7±0.2°K, respectively.

In summary, the M-versus-T relation for Rb_2MnF_4 is quite similar to that observed in K_2NiF_4. In both cases a power law gives a good description of the data at all temperatures although at low temperatures this seems to be fortuitous. Fits to the data for $1-T/T_N<10^{-1}$, that is, within the "critical region," give $B=0.96\pm0.06$, 0.98 ± 0.03 and $\beta=0.16\pm0.02$, 0.14 ± 0.01 in Rb_2MnF_4 and K_2NiF_4, respectively. The B parameters are anomalously small in both cases while the β's are quite close to the [2] $S=\frac{1}{2}$ Ising value.

3. Rb_2FeF_4

In Sec. IV B *3* we saw that the Rb_2FeF_4 Bragg peak intensity changed in a smooth continuous manner around T_N rather than in the sharp quasidiscontinuous manner characterizing the K_2NiF_4 and Rb_2MnF_4 phase transitions. It is clear, therefore, that an interpretation of the Bragg intensity in terms of the sublattice magnetization will be more complicated in this compound. In Fig. 15, the temperature variation of the (1,0,0), (0,1,3), (1,0,4) peak intensities are shown. At about 44°K the intensities of the (0,1,3) and (1,0,4) peaks actually cross over. However, the relative intensities of the (1,0,0) and (1,0,4) reflections, both of which arise from the same domain, is a constant over the temperature range 4.2–55°K. Measurements of the (0,3,1) peak intensity at 52.6°K show that it is two orders of magnitude smaller than (3,0,0), thus necessitating that the spin still point directly along the b axis at this temperature. This leads one to conclude that the

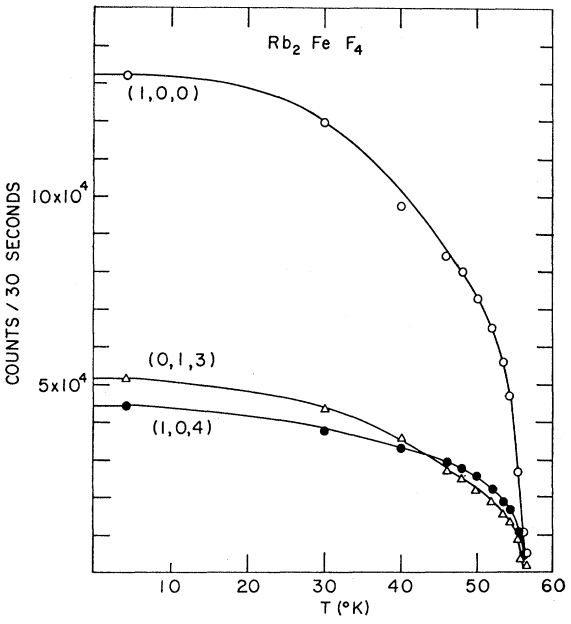

FIG. 15. Intensity variation in Rb_2FeF_4 of the (1,0,0), (0,1,3), and (1,0,4) rl positions as a function of temperature.

change in relative intensities of the (0,1,3) and (1,0,4) peaks with temperature is due solely to a change in relative *populations* of the two domains. No such effect was observed in either K_2NiF_4 or Rb_2MnF_4. No attempt was made to investigate this effect in detail although it was observed that the relative populations of the two domains at a given temperature seemed to change on cycling through $T_N=56.3$°K. The general shape of Fig. 15, however, seemed to be reproducible.

In order to deduce the true M-versus-T relationship from the data in Fig. 15, it is necessary to remove the effects of the shift in domain populations. It is straightforward to show that this is accomplished by using the linear combination $I(0,1,3)+0.906I(1,0,4)$, where 0.906 is the calculated ratio of the two peak intensities for equal populations. The results of this analysis are shown in Fig. 16. The magnetization curve is found to have a very different form from the simple straight lines characterizing the K_2NiF_4 and Rb_2MnF_4 $\log M$-versus-$\log T$ relationships (Figs. 12 and 14). Over the range from about $2\times10^{-2}<1-T/T_N<0.3$, $\log M$ is approximately linear with $\log T$ with a slope of $\beta\simeq0.2$. However, the slope increases rapidly as the phase transition is approached. This change may arise either from a fundamental change in the critical behavior of Rb_2FeF_4 or else from an extraneous effect such as a distribution of Néel temperatures. We shall discuss these results in more detail in Sec. V.

C. Inelasticity

In Sec. IV A, we have discussed the ridge scattering for $T>T_N$ in terms of [2] critical scattering. This description of the ridge was based on the temperature

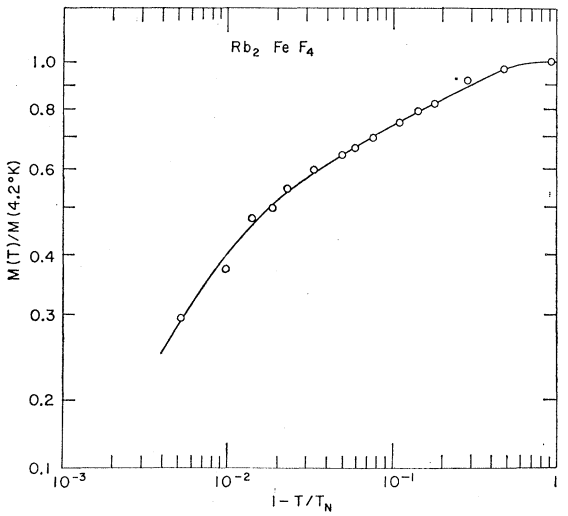

FIG. 16. Rb_2FeF_4 sublattice magnetization deduced from the data in Fig. 15 in the manner discussed in the text.

evolution of both the rod intensity and linewidth. It is, however, possible that the ridge for $T>T_N$ could arise from some complicated [2] Bragg process. This question may be simply answered by energy analyzing the ridge since by definition the critical scattering must be inelastic, as discussed in Sec. III A. For experimental reasons, it was most convenient to carry out the inelastic measurements on Rb_2FeF_4. However, the results will most certainly be valid for all three compounds.

The measurements were carried out on a triple-axis spectrometer using neutrons of wavelength 2.618 Å. The monochromator and analyzer were, respectively, germanium (1,1,1) and (2,2,0). The system had 20′ collimators before the monochromator and detector and 40′ collimation before and after the sample. The energy analysis was carried out in the constant-Q mode of operation. Most measurements were made at (1, 0, −0.5) since at this position the resolution ellipse was oriented such that $\mathbf{q}_{[2]}$ was as sharply defined as possible.

The results of the energy scans at (1, 0, −0.5) are listed in Table VII. In the immediate neighborhood of $T_N\simeq56.3$°K, the scattering has the form of a sharp Gaussian peak with full width at half-maximum of ∼0.35 meV. This is approximately the width expected for the resolution function alone. As the temperature is

TABLE VII. Energy analysis of Rb_2FeF_4 ridge at (1, 0, −0.05).

T(°K)	ΔE (meV)
56.0	0.35±0.05
56.2	0.36±0.05
56.7	0.40±0.05
57.0	0.41±0.05
64.1	0.78±0.05
70.0	1.6 ±0.1

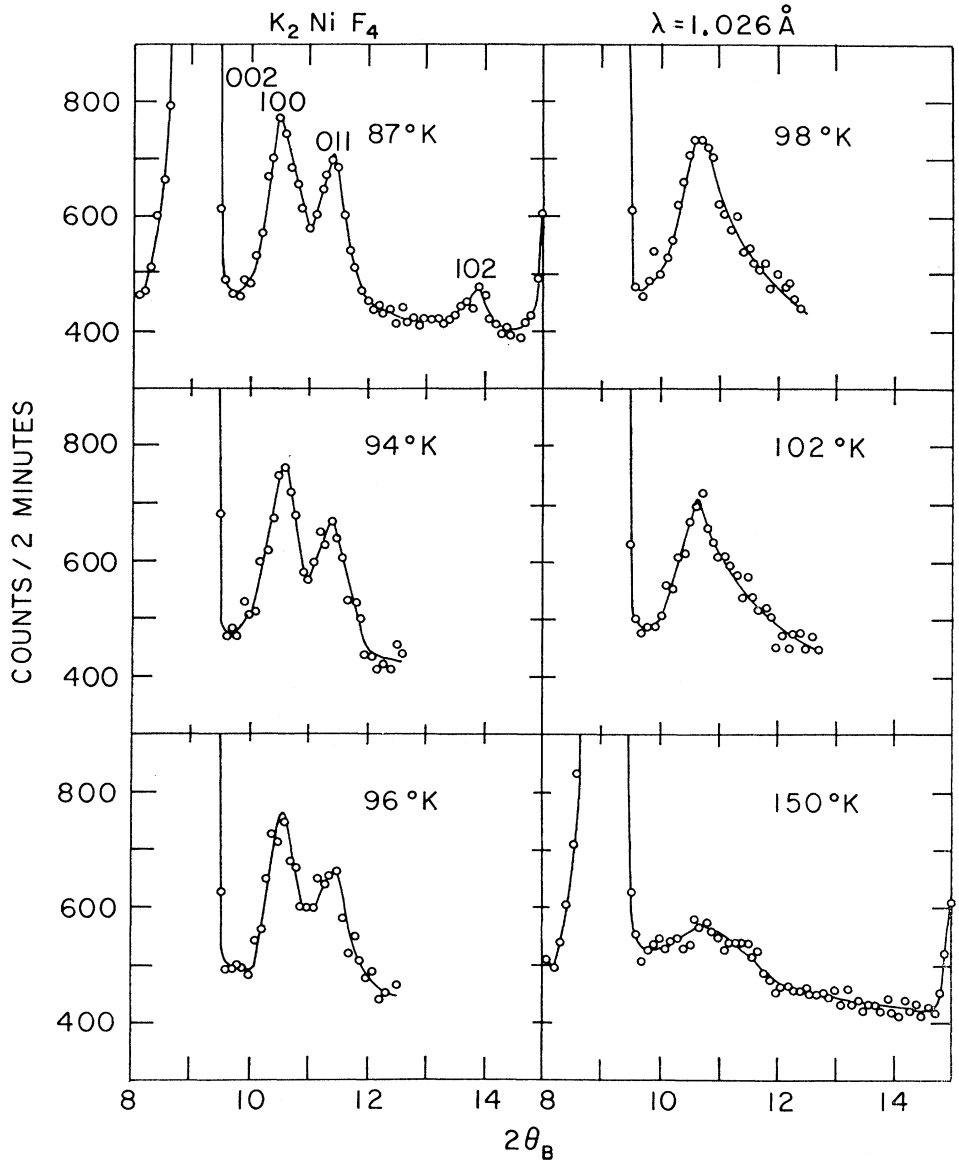

FIG. 17. Temperature evolution of K_2NiF_4 powder neutron diffraction pattern in the neighborhood of the (1,0,0) magnetic peak.

increased above T_N the peak broadens, thus indicating that for $T > T_N$ the ridge has an intrinsic energy width, that is, it is *inelastic*. We conclude, therefore, that the ridge results from genuine [2] critical scattering. The decrease in inelasticity as the phase transition is approached is just the critical "slowing down" of the spin fluctuations which has been observed in a number of [3] systems.[31]

D. K_2NiF_4 Powder Measurements

Much of the difficulty in understanding the early work on these [2] systems arose from the apparent discrepancies between the powder neutron diffraction results and bulk property measurements.[4,6,7] It is interesting, therefore, to reconsider the powder measurements in light of our detailed knowledge of the [3] form of the scattering. Indeed, as noted previously, it was just such a reconsideration which led the authors to a better understanding of the single-crystal work.

The temperature evolution of the innermost magnetic powder peaks is shown in Fig. 17. At 87°K, the (1,0,0), (0,1,1), and (1,0,2) peaks arising from the magnetic structure shown in Fig. 2 are well defined. The relative intensities, however, differ considerably from those expected from theory. A comparison with the nuclear peaks shows that this apparent discrepancy arises from extreme preferred orientation of the crystallites which, as might be expected, tend to have a platelet shape. As the temperature is increased from 87°K towards $T_N = 97.1$°K there is little change in the magnetic peaks. However, as the temperature is increased from 96°K through T_N to 98°K the (0,1,1) and (1,0,2) peaks seem

to disappear while the (1,0,0) peak shows no apparent change. The explanation of this phenomenon is quite straightforward. Above 97.1°K there is no [3] LRO so there can be no sharp [3] peaks. However, there are still considerable [2] correlations which give rise to appreciable scattering intensity in the form of a ridge along (1,0,l). The powder pattern arising from such a ridge is, in fact, just that observed at 98°K. The minimum $2\theta_B$ for the ridge around T_N is just $2\theta_B(1,0,0)$. Furthermore, in the region around (1,0,0), $2\theta_B$ for the rod has no first-order dependence on $|l|$ so that the powder measurement effectively integrates over a large section of the ridge. This then gives rise to a sharp peak at $2\theta_B(1,0,0)$ with a tail that extends in the direction of increasing $2\theta_B$. An empirical demonstration of this may be seen in Fig. 5. The upper part of the figure corresponds to a wide-angle φ scan along the ridge around (1,0,0) with $2\theta_B$ fixed at $2\theta_B(1,0,0)$. Although the scattering intensity is down by nearly two orders of magnitude from the (1,0,0) Bragg peak intensity at low temperatures, the linewidth is much larger so that the integrated intensities are comparable. The integrated intensity at (0,1,3), however, is much weaker as expected.

The peak at (1,0,0) decreases in intensity with increasing temperature in a manner dictated by $\chi(\mathbf{q})$. From the single-crystal work it was found that there are appreciable correlations up to nearly $2T_N$ and indeed the (1,0,l) ridge powder peak is also discernible up to that temperature. In general, therefore, the powder measurements contain considerable information about both the [2] and [3] aspects of the system. They should prove quite useful in an initial characterization of systems for which single crystals are available and also they may provide valuable information about the possible existence of [2] correlations even in systems for which only powders are available.

V. DISCUSSION AND CONCLUSIONS

A review of the experimental results in Sec. IV shows that the three compounds K_2NiF_4, Rb_2MnF_4, and Rb_2FeF_4 exhibit a wide variety of properties which are radically different from conventional [3] antiferromagnets. In each case, there is a wide temperature range over which there are appreciable [2] correlations with no evidence of any [3] behavior at all. The planes at these temperatures are totally isolated from each other magnetically and are behaving as bonafide [2] antiferromagnets in the paramagnetic phase. In K_2NiF_4 and Rb_2MnF_4, the ridge intensity increases while its linewidth concomitantly decreases with decreasing temperature until they both reach a limiting value at a temperature we designate T_N. At this same temperature [3] Bragg peaks appear but with no accompanying [3] critical scattering observed on approaching the phase transition from either above or below. The only plausible explanation of this behavior is that in both K_2NiF_4 and Rb_2MnF_4 the phase transition is a *genuine [2] phase transition*. By this we mean that the system achieves LRO solely because of the [2] properties; loosely speaking, one may envisage the system as achieving LRO in two dimensions and then by necessity ordering in three dimensions since even a microscopic interaction between nnn planes is then amplified by N, the number of spins in a plane. A more precise description of the phase transition probably requires one to envisage the system as having two critical regions. The first, which is purely [2] in form and which is the only one we have been able to monitor experimentally, corresponds to the growth of the correlations within the planes. At some point, the correlation length within the planes must become sufficiently long (perhaps macroscopic) that these spin "globules" in the different nnn planes become aware of each other's existence. At this temperature, the critical behavior must go over to being [3] in character. However, in terms of absolute temperature this [3] region may be extremely small and indeed we have been unable to obtain any experimental evidence for its existence in either K_2NiF_4 and Rb_2MnF_4. Most importantly, the [3] aspects of the system do not seem to alter the pure [2] nature of the phase transition for values of $|1-T/T_N|$ down to at least 10^{-3}. Indeed, the lack of importance of the [3] properties is dramatically illustrated in Rb_2MnF_4 where the two distinct [3] LRO phases have indistinguishable magnetization curves.

We have been able to obtain values for the critical parameters B, β in $M(T)/M(4.2°\text{K})=B(1-T/T_N)^\beta$ for K_2NiF_4 and Rb_2MnF_4. In the region $\sim 10^{-3}<1-T/T_N<10^{-1}$ they are given by $B=0.98$, $\beta=0.14$ in K_2NiF_4 and $B=0.96$, $\beta=0.16$ in Rb_2MnF_4. The values for β are both much closer to the [2] $S=\frac{1}{2}$ Ising value of $\frac{1}{8}$ than conventional [3] values of approximately $\frac{1}{3}$. In general, one expects that although critical exponents may vary somewhat for different interaction models their general magnitudes are characteristic of the dimensionality. The low values of β which we observe, therefore, are quite consistent with our identification of the critical behavior as being entirely [2]. An alternative way of picturing the magnetization is to imagine that we have a series of [2] antiferromagnets (N' in all) stacked on top of each other such that $\langle S_z\rangle_{[2]}$ for the planes sums. The [3] order then conveniently enables us to measure $N'\langle S_z\rangle_{[2]}$ but plays no role in the thermal evolution of $\langle S_z\rangle_{[2]}$.

One of the most fascinating features of the magnetization measurements is the fact that a simple power law holds at all temperatures. However, the good agreement which one obtains using simple spin-wave theory up to $0.8T_N$ in K_2NiF_4 and up to at least $0.6T_N$ in Rb_2MnF_4 would seem to indicate that it is simply a strange coincidence. Indeed, the fact that spin-wave theory works over such a wide temperature range is itself quite unusual. This can be partially understood by noting

TABLE VIII. Phase-transition temperatures.

	Experiment (°K)	Stanley-Kaplan (°K)	Anisotropy-induced (°K)
K_2NiF_4	97.1	90	106
Rb_2MnF_4	38.4	34	33
Rb_2FeF_4	56.3	43	···

that the spin waves involved still have relatively long wavelengths even at $0.8T_N$ due to the fact that T_N is depressed relative to the magnon zone boundary energy. This depression in turn, arises from the [2] near-Heisenberg nature of the system. However, one must be cautious in making too explicit statements, since one might equally well claim that the agreement with spin-wave theory is a coincidence and the system is really "critical" down to at least $0.5T_N$.

As noted previously, the values we obtain for B are also anomalously small. However, this can be understood in at least a qualitative fashion by reference to Fig. 12. If we compare the K_2NiF_4 magnetization curve with the [2] Ising curve, we see that the major difference is that the latter saturates at about $1-T/T_N=0.4$ whereas the former is still increasing in the manner illustrated in Fig. 13. This difference arises from the fact that the [2] Ising model has no low-energy excitations, that is, magnons, so that there is almost no diminution of the magnetization at low temperatures. The effect of thermally populated magnons in K_2NiF_4 is to lower B. Indeed, the system might be thought of as a near-Heisenberg system which then goes critical like a [2] Ising model.

Most of the above features are also present in Rb_2FeF_4. However, within about 1°K of either side of the phase transition there is a gray area in which the system seems to have simultaneously [2] and [3] properties. This is shown clearly in Figs. 9, 10, 16. There are two possible explanations of this behavior. The first, which has the most physical appeal, is that Rb_2FeF_4 is more [3] in its behavior due to the magnetostrictive distortion which serves to couple nn planes. The gray area then would be that range in $|1-T/T_N|$ in which the phase transition had gone over to being [3] in character. A second explanation, which in fact is one offered by the Mössbauer group, is that there is a spread in T_N of about 2°K. These two hypotheses are difficult to differentiate between experimentally. We have made some initial attempts but they have not been totally successful. More detailed studies of the ridge and Bragg peaks in the immediated neighborhood of T_N are required before this question can be unambiguously answered.

So far we have not posed the question of whether the [2] phase transition is the anisotropy-induced transition of Lines or the more esoteric Stanley-Kaplan isotropic transition referred to in the Introduction. Stanley and Kaplan[2] have derived the expression

$$kT_{SK}=\tfrac{1}{10}J(z-1)[2S(S+1)-1] \qquad (20)$$

for the two-dimensional ferromagnet. Stanley[37] also reports that this mnemonic formula is a good approximation for the [2] isotropic antiferromagnet. Using the exchange constants given in Sec. II we obtain the values given in Table VIII for T_{SK}. The corresponding values for the anistropy-induced phase transition as calculated by Lines[38] are also given in the table. The agreement for both theories is reasonable and, considering their approximate nature it is impossible to decide on the basis of T_N alone which mechanism is in fact responsible. However, we have found that below T_N all three systems have conventional [3] LRO. This is consistent with Lines's anisotropy model but would seem to require a reformulation of the Stanley-Kaplan picture. We conclude, therefore, that Lines's anisotropy model is the more reasonable description of the phase transition. It is quite remarkable that in K_2NiF_4, 1°K of anisotropy is apparently sufficient to raise the ordering temperature from 0 to 97.1°K.

Our original aim in this study was to carry out a groundwork survey of the properties of the planar antiferromagnets K_2NiF_4, Rb_2MnF_4, Rb_2FeF_4. From the data, we have been able to conclude that these crystals exhibit the first [2] magnetic phase transitions found in nature. The transitions seem to be rather complicated in their details but over-all they have an aesthetically pleasing simplicity. It is clear that detailed study of the static and dynamic properties of these systems in the neighborhood of the phase transition could yield results of considerable importance to our understanding of cooperative phenomena.

ACKNOWLEDGMENTS

We have benefitted immensely from discussions of this work with B. I. Halperin, P. C. Hohenberg, M. E. Lines, and L. R. Walker of Bell Telephone Laboratories, and M. Blume and J. Skalyo, Jr., of Brookhaven. We are also indebted to S. J. Pickart and H. E. Stanley for valuable advice.

[37] H. E. Stanley, J. Appl. Phys. **40**, 1546 (1969).
[38] M. E. Lines (private communication).